Accepted Manuscript

Discovery of chalcone-modified estradiol analogs as antitumour agents that Inhibit tumour angiogenesis and epithelial to mesenchymal transition

Cong Wang, Leilei Li, Dongyang Fu, Tiantian Qin, Yange Ran, Feng Xu, Xinrui Du, Haiying Gao, Shuaijun Sun, Tengjiao Yang, Xueyan Zhang, Junfeng Huo, Wen Zhao, Zhenzhong Zhang, Xiufang Shi

PII: S0223-5234(19)30399-X

DOI: https://doi.org/10.1016/j.ejmech.2019.04.071

Reference: EJMECH 11306

To appear in: *European Journal of Medicinal Chemistry*

Received Date: 7 December 2018

Revised Date: 29 April 2019

Accepted Date: 29 April 2019

Please cite this article as: C. Wang, L. Li, D. Fu, T. Qin, Y. Ran, F. Xu, X. Du, H. Gao, S. Sun, T. Yang, X. Zhang, J. Huo, W. Zhao, Z. Zhang, X. Shi, Discovery of chalcone-modified estradiol analogs as antitumour agents that Inhibit tumour angiogenesis and epithelial to mesenchymal transition, *European Journal of Medicinal Chemistry* (2019), doi: https://doi.org/10.1016/j.ejmech.2019.04.071.

Discovery of Chalcone-Modified Estradiol Analogs as Antitumour Agents that Inhibit Tumour Angiogenesis and Epithelial to Mesenchymal Transition

Cong Wang [a], Leilei Li [a], Dongyang Fu [a], Tiantian Qin [a], Yange Ran [a], Feng Xu [a], Xinrui Du [b], Haiying Gao [a,c], Shuaijun Sun [a,d], Tengjiao Yang [e], Xueyan Zhang [a], Junfeng Huo [a], Wen Zhao [a], Zhenzhong Zhang [a], Xiufang Shi [a]*

[a] Collaborative Innovation Center of New Drug Research and Safety Evaluation, Henan Province; Key Laboratory of Advanced Drug Preparation Technologies, Ministry of Education; Key Laboratory of Henan Province for Drug Quality and Evaluation; School of Pharmaceutical Sciences, Zhengzhou University, Zhengzhou 450001, P. R. China

[b] Department of Clinical Medicine，Zhengzhou University, 40 Daxue Road, Zhengzhou, Henan 450052, China

[c] Department of Pharmacy, People's Hospital of Daqing, 241 Jianshe Road, Development District, Daqing 163316, Heilongjiang, China.

[d] Department of Pharmacy, Zhengzhou Central Hospital Affiliated to Zhengzhou University, 195 Tongbai Road, Zhengzhou 450053, Henan, China

[e] HeNan No.3 Provincial People's Hospital, Funiu Road, Zhongyuan District, Zhengzhou 450000, Henan, China

*Corresponding author at: School of Pharmaceutical Sciences, Zhengzhou University, 100 Kexue Avenue, Zhengzhou, Henan 450001, PR China. E-mail address: xfxiu@zzu.edu.cn (X.Shi), wangcong@zzu.edu.cn (C Wang)

Abstract

Angiogenesis plays an essential role in tumourigenesis and tumour progression, and anti-angiogenesis therapies have shown promising antitumour effects in solid tumours. 2-Methoxyestradiol (2ME2), an endogenous metabolite of estradiol, has been regarded as a potential antitumour agent mainly targeting angiogenesis. Here we synthesized a novel series of chalcones based on 2-methoxyestradiol and evaluated their potential activities against tumours. Compound **11e** was demonstrated to have potent antiangiogenic activity. Further studies showed that **11e** suppressed tumour growth in human breast cancer (MCF-7) xenograft models without obvious side effects. Evaluation of the mechanism revealed that **11e** targeted the epithelial to mesenchymal transition (EMT) process in MCF-7 cells and inhibited HUVEC migration and then contributed to hindrance of angiogenesis. Thus, **11e** may be a promising antitumour agent with excellent efficacy and low toxicity.

Keywords: 2-methoxyestradiol, antitumour, angiogenesis, EMT, migration

Graphical abstract

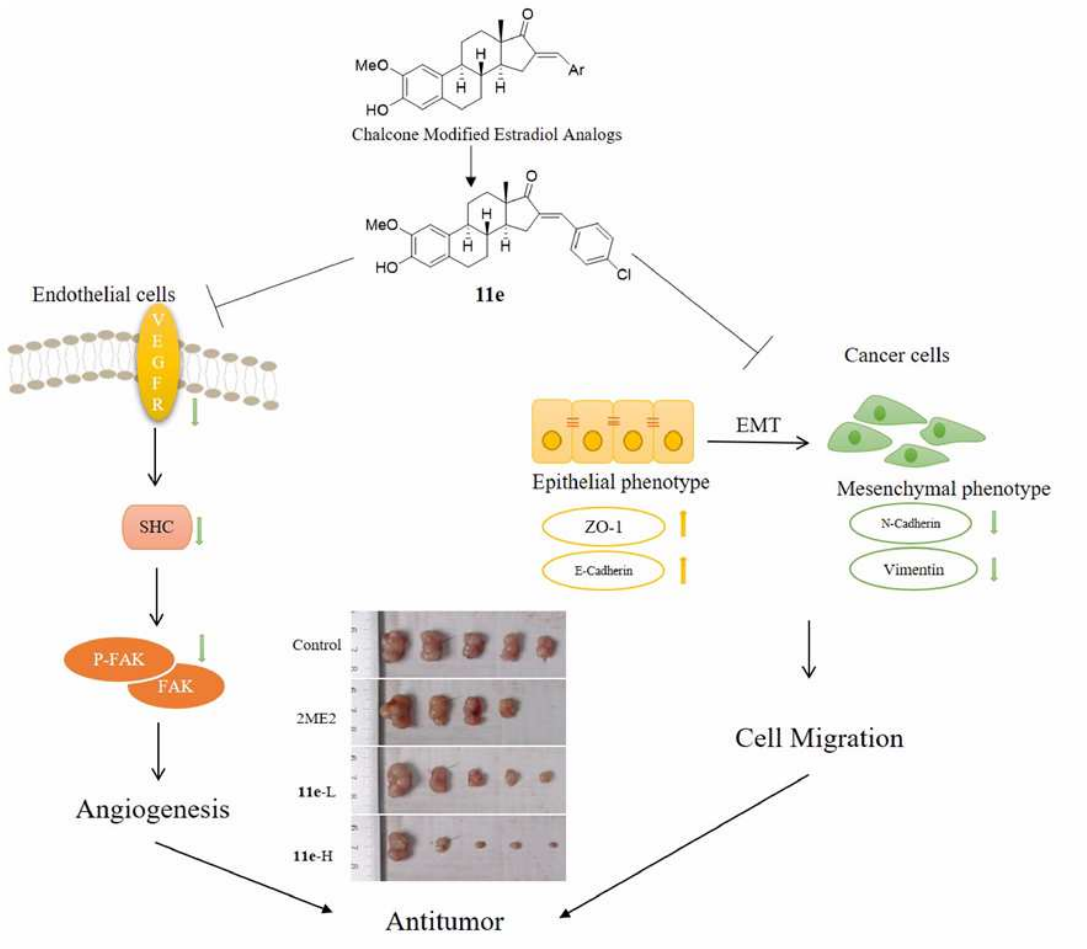

Introduction

Angiogenesis, the formation of new blood vessels from the pre-existing vessels, has been described as one of the hallmarks of cancer. It plays an essential role in tumour growth, invasion, and metastasis[1-3]. Tumour angiogenesis occurs when the cancer cells stimulate new blood vessel growth in order to bring oxygen and nutrients to a tumour[4, 5]. As a tumour grows in size, diffusion is no longer sufficient to oxygenate the cells at the centre of the mass and a hypoxic environment is created[6, 7]. Cancer cells secrete a variety of growth factors and cytokines that stimulate the classical angiogenic signalling pathways, extracellular matrix remodelling, and an inflammatory response that lead to new blood vessel formation[8-10]. Vascular endothelial growth Factor (VEGF) is known as the most important growth factor that binds to VEGFR2, VEGFR1, and VEGFR3 tyrosine kinase receptors on the endothelial cell surface,

which promotes proliferation and migration of endothelial cells[11, 12]. Some signalling pathways also take part in angiogenic response including PI3K/Akt, Wnt, and Notch[12-14].

Extensive efforts are directed towards antiangiogenic therapies that combat cancer by preventing it from accessing the blood supply that is critical for tumour growth and survival[15-17]. The antiangiogenic inhibitors approved by the FDA can be divided into 3 categories: (1) monoclonal antibodies designed to target specific pro-angiogenic factors and receptors, e.g. Bevacizumab directed against vascular endothelial growth factor (VEGF) used for colorectal and lung cancer[18]; (2) tyrosine kinase inhibitors(TKI) to target receptors of multiple proangiogenic factors, e.g. sorafenib treatment for advanced renal cell carcinoma[19]; (3) mTOR inhibitors (mammalian target of rapamycin inhibitors), e.g. everolimus reduced tumor volume and angiogenesis in Hepatocellular carcinoma (HCC) mouse models[20, 21]. Although antiangiogenic therapy made certain progress in prolonging the survival of cancer patients, there are still only a few satisfactory results because of certain limitations including insignificant clinical effects, concerns about safety, tumour recurrence and drug resistance[22, 23]. Therefore, the development of novel, safer and multi−targeted inhibitors is urgently required.

2ME2 is derived from the NADPH−dependent cytochrome P450 metabolism of 17β-estradiol. 2ME2 is an endogenous metabolite with antiangiogenic and antitumour effects[24]. The antiangiogenic effect is mainly due to inhibition of cell adhesion and migration, induction of apoptosis of vascular endothelial cell and inhibition of vascular endothelial growth factors and hypoxic-inducible factor (HIF)[25]. Additionally, 2ME2 combats cancer by targeting tubulin polymerization via binding at the colchicine-binding site and arresting cell cycle at G2/M-phase. Several phase Ⅰ and Ⅱ clinical studies have been conducted to evaluate 2ME2 under the name of Panzem®, a formulation in a nanocrystal colloidal dispersion (NCD®), in multiple myeloma, glioblastoma ovarian and prostate cancers [26-28]. However, the short half-life and poor bioavailability of 2ME2 limited its clinical applications[24, 29]. New analogs STX140 and ENMD-1198 were demonstrated to have potentially higher anticancer activities than that of 2ME2. These compounds are being evaluated in Phase I/Phase Ⅱ clinical trials[30, 31]. Research demonstrated STX140 inhibited the proliferation of MCF-7 cells and caused arrest in the G2/M phase of the cell cycle[32], and latest research shows that STX140 can target CA Ⅸ which is regarded as a potential treatment target in triple-negative breast cancer (TNBC)[33], ENMD-1198 inhibited HIF1-a, but it also decreased STAT3 and NF-kB levels in breast and prostate cancer[34]. Chalcones are the derivatives of (*E*)-1,3-diphenyl-2-propene-1-one and represent a class of compounds consisting of two aryl rings linked by an α,β-unsaturated ketone moiety. It's reported that chalcones possessed anticancer activity by preventing tubulin polymerization[35]. Various chalcone-modified steriod derivatives were synthesized and some of the derivatives showed potent anticancer activity against certain human cancer cell lines[36], for example the chalcone with a trimethoxyphenyl unit (**1**) was considered as potential cytotoxic effect and antitubulin activity, 2-chalcone substituted 17-methylene estratriene (**2**) exhibited highly antiproliferative activity against colon

HCT-116, lung NCIH-460, glioma U-251 and breast MDA-MB-435 cancer cells (GI_{50}=1.6 μM, 2.6 μM, 1.4 μM, 1.6 μM)[37], 16-*E*-arylidene and rostenes (**3**) were demonstrated potential anticancer agent against CCRF-CEM, K-562, RPMI-8226 and SR leukemia cell lines (GI_{50}=3.94 μM, 2.61 μM, 6.90 μM, 1.79 μM)[38]. 17-chalconyl pregnenolones exhibited the highly activity against MCF-7 and MDA-MB-231 (IC_{50}=2 μM)[39]. and estrone-16-oxime (**4**) showed highly cytotoxic effect against HeLa cells (IC_{50}=4.41 μM)[40]. (**Fig. 1**)

However, synthesis of chalcones on 2-methoxyestradiol (2ME2) has not been studied so far. In order to further explore the SAR of 2ME2 and enrich the structure types of the chalconyl steroid compounds, we first synthesized 2-chalconyl estradiol analogs using 2-acetyl-estradiol-17β-acetate as the steroid precursor. The 2-acetyl group of estradiol was used to form α,β-unsaturated carbonyl moiety with different aldehydes according to Claisen-Schmidt condensation, which chalcone unit differs from the reported lies in the positions of carbonyl and double bond[26]. We also prepared a novel class of D-ring chalcone-modified 2-methoxyestradiol analogs and evaluated the antiproliferative activity, antiangiogenic activity and anti-metastasis effect on MCF-7. We found that compound **11e** is a multi-target compound, which has a good effect on inhibiting angiogenesis and anti-migration of MCF-7 in breast cancer.

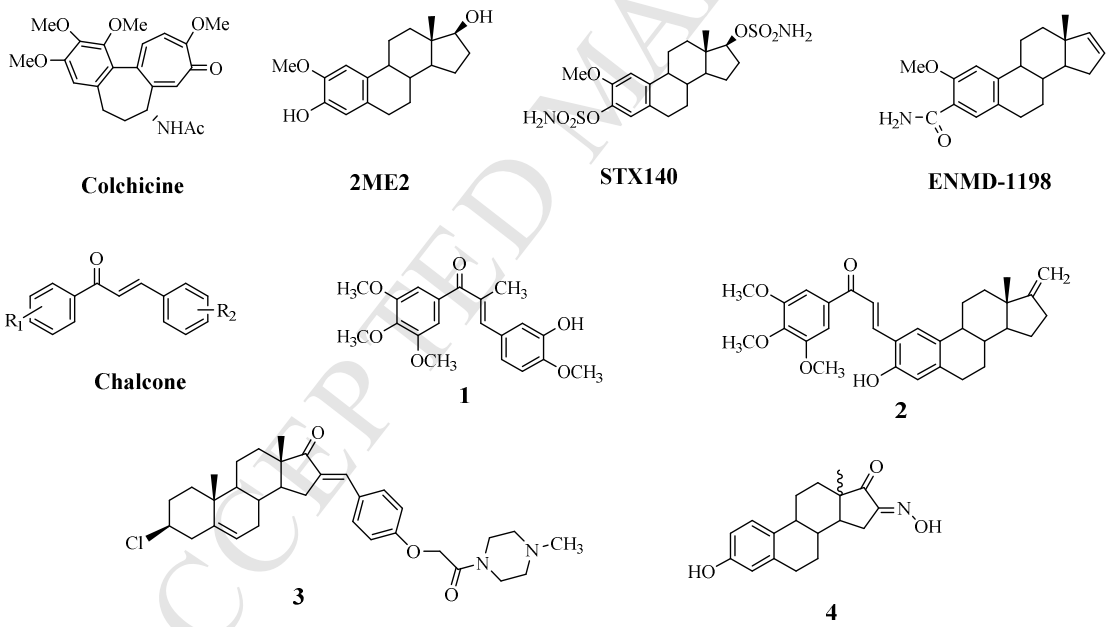

Fig. 1. Colchicine, 2ME2 and 2ME2 analogs, chalcone and chalcone steroid analogs

Results

Chemistry.

The synthesis route of the target 2-benzylideneacetyl substituted 17β-estradiol compounds is depicted in **Scheme 1**. Chalcone moiety was synthesized from aldehyde and acetophenone according to Claisen-Schmidt condensation. Saxena[41] and Panchapakesan[37] reported 2-aroylvinyl-substituted 17β-estradiol synthesis from a 2-formyl estradiol substrate and various acetophenones. Here, 2-acetyl-estradiol-17β-acetate (**6**) was prepared by esterification using the Fries rearrangement with estradiol as the starting material based on Rao's method[42]. Then, different substituted aromatic aldehydes were employed in the Claisen-Schmidt condensation to obtain various 2-benzylideneacetyl-substituted 17β-estradiol compounds. The overall yield of 2-chalcone estradiol (**7**) from estradiol was 52%~64%.

The 2-chalcone moiety was shown to be in the trans-configuration of the double bond according to the coupling constant (J) values of 15.4-15.7 Hz. In the ^{1}H NMR spectrum of compounds, two protons of the propenone moiety were observed as two doublets at δ 7.81~8.26 (CH=C-CO) and 7.47~7.76 ppm (=CH-CO). In the ^{13}C NMR spectrum, the ketone carbonyl groups were detected at 192.90-193.99 ppm and the vinylic carbons C-20 and C-21 were observed as the chemical shift at 118.21-123.51 and 139.93-147.83 ppm, respectively, indicating the presence of α,β-unsaturated ketones. The *E*-conformation in the α,β-unsaturated ketone in the 2-chalcone steroid were further supported by X-ray crystal structure of **7e (Fig. 2a)**. The α,β-unsaturated ketone system is characterized by C19=O2 and C20-C21 bond lengths of 1.243(3) and 1.319(4) Å and a torsion angle O2-C19-C20-C21 of 4.6(5)˚, H20-C20-C21-H21 of 176.67˚(Mercury version 3.10). The date are consistent with the studies of other chalcone derivatives reported previously[41, 43].

The synthesis of various 16*E*-arylidenoestraene derivatives has been carried out as depicted in **Scheme 2**. 2ME2 was synthesized from commercially available estradiol as described in a literature[42]. The C3-OH of 2ME2 was then selectively acetylated by using acetic anhydride in isopropanol to afford **8** with 95% yield. Subsequent Jones oxidation followed by base hydrolysis gave 2-methoxyestrone (**10**) at 82% overall yield. Finally, the Claisen-Schmidt reaction of 2-methoxyestrone with the corresponding benzaldehyde derivatives at room temperature in the alkaline medium afforded 16*E*-benzylidene-substituted 2-methoxyestrone derivatives **11a-l**. The intermediates **8-10** can be conveniently purified by crystallization. The overall yield of 16*E*-benzylidene 2-methoxyestrone (**11**) from 2-methoxyestradiol was approximately 68%. We adopted a one-pot reaction; compound **10** did not need separation and following Claisen-Schmidt reaction was performed immediately using benzaldehyde to obtain16*E*-benzylidene 2-methoxyestrone (**11**). The overall yield of **11** was increased by 78%.

The ^{1}H NMR signal of the methine-H was found the downfield region at 7.36 to 7.81 ppm for the *E*-isomer **11** as expected due to deshielding caused by proximity to the carbonyl group in agreement with the literature [37]. In the ^{1}H NMR spectrum of compounds **11a~11l**, 16-arylidene hydrogen is a singlet at approximately 7.48 ppm, but it becomes a doublet in **11c** due to the splitting of fluorine. In the ^{13}C NMR spectrum, the expected signal for a ketone carbonyl at 208.81–209.74 and the vinylic carbons C-16 and C-20 at 131.25–141.02 ppm indicated the presence of α,β-unsaturated ketones. This observation has been confirmed by the X-ray diffraction analysis of **11c (Fig. 3b)**. The α,β-unsaturated ketone system is characterized by C17=O3 and C16-C20 bond lengths of 1.207(4) and 1.341 Å (5) Å, respectively, and a torsion angle C17-C16-C20-C21 of -179.0˚ (3). These properties are very similar to those observed in two related arylidene derivatives of estrone[44].

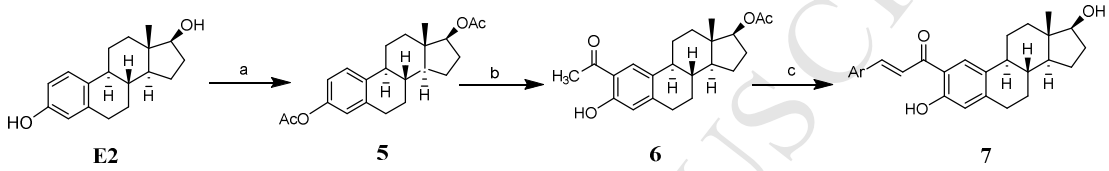

E2 **5** **6** **7**

compound	Ar	compound	Ar
7a	2-methoxyphenyl	**7e**	2-chlorophenyl
7b	3-methoxyphenyl	**7f**	3-chlorophenyl
7c	4-methoxyphenyl	**7g**	4-chlorophenyl
7d	4-benzyloxyphenyl	**7h**	2,4-dichlorophenyl

Scheme 1 Synthesis of 2-chalconyl substituted estradiol derivatives.
Reagents and conditions: (a) Ac_2O, Pyridine, 60 ℃; (b) $ZrCl_4$, CH_2Cl_2, N_2, rt; (c) aromatic aldehyde, 95% EtOH, 10% NaOH, 60 ℃.

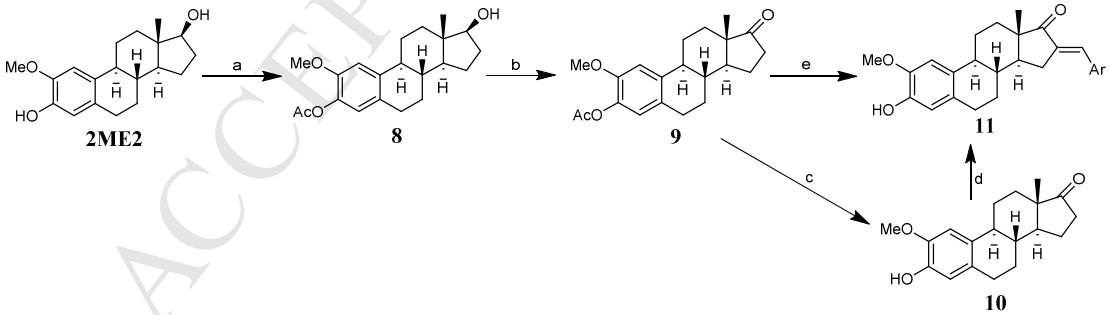

2ME2 **8** **9** **11** **10**

compound	Ar	compound	Ar
11a	phenyl	**11g**	4-bromophenyl
11b	4-fluorophenyl	**11h**	3-nitryphenyl
11c	3,4-difluorophenyl	**11i**	4-methylsulfonatephenyl
11d	3-chlorophenyl	**11j**	4-methylphenyl
11e	4-chlorophenyl	**11k**	2,3-bimetyoxyphenyl
11f	2,4-dichlorophenyl	**11l**	3,4,5-trimethoxyphenyl

Scheme 2. Synthesis of 16-benzylidene-substituted 2-methoxyestrone derivatives Reagents and conditions: (a) Ac_2O, isopropanol, rt; (b) Jones reagents, 0 □; (c) 10% NaOH, MeOH; (d) aromatic aldehyde, EtOH, 10% KOH, rt; (e) aromatic aldehyde, EtOH, 10% KOH.

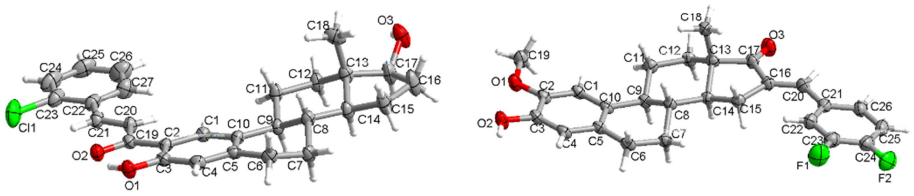

a b

Fig. 2. X-ray crystal structure of **7e** (a) and **11c** (b)

Biological Testing

The effect of 2ME2 derivates on cytotoxicity *in vitro* and angiogenesis *in vivo*

All 20 analogs were screened for antitumour activities against six different cancer cell lines including SKN-SH (Neuroblastoma), B16 (Melanoma, skin), A549 (Lung adenocarcinoma), MGC-803 (Gastric cancer), EC109 (Esophageal carcinoma) and SMMC-7721 (Hepatocellular carcinoma) cells *in vitro*, The percentage of growth inhibition was assessed using SRB assay. The 50% growth inhibitory concentration (IC_{50}) were determined and listed in **Table 1**. The results indicated that most of the synthesized compounds showed moderate cytotoxic activity in all six cell lines.

Table 1 Cytotoxic activity of 2- or 16- chalcone substituted estradiol analogs

Drug	IC_{50}(μM)					
	SKN-SH	B16	EC-109	MGC-803	A549	SMMC-7721
2ME2	1.6±1.2	3.4±0.6	4.1±0.8	4.0±0.9	1.1±0.0	8.4±0.9
7a	22.2±1.3	16.5±1.2	26.5±1.4	9.8±1.0	5.9±0.8	0.6±0.3
7b	4.5±0.6	8.9±0.9	5.6±0.7	4.0±0.6	5.5±0.8	26.1±1.5
7c	18.9±1.2	17.4±1.2	18.2±1.3	12.2±1.1	8.6±0.9	16.1±1.0
7d	>128	>128	>128	>128	52.6±1.7	>128
7e	16.4±1.2	15.9±1.2	13.2±1.1	8.3±0.9	15.5±1.2	11.3±1.1
7f	10.3±1.0	12.4±1.1	8.5±0.9	8.0±0.9	10.9±1.0	6.3±0.8

7g	15.0±1.1	15.3±1.2	14.0±1.2	15.7±1.1	12.1±1.1	44.9±1.1
7h	22.7±1.4	13.1±1.1	19.4±1.3	12.5±1.1	13.7±1.1	14.5±1.2
11a	22.4±1.4	17.8±1.3	22.8±1.6	17.7±1.2	19.4±1.1	17.2±1.5
11b	27.0±1.4	16.8±1.2	19.9±1.3	13.5±1.1	25.3±1.4	8.2±1.0
11c	8.0±1.3	14.2±1.3	16.2±1.2	10.7±1.0	15.0±1.2	5.1±1.7
11d	21.0±1.3	10.1±1.0	24.3±1.3	12.3±1.1	22.6±1.3	16.9±1.1
11e	24.7±1.4	17.9±1.3	14.7±1.2	14.9±1.2	23.2±1.4	4.3±1.0
11f	17.8±1.2	16.5±1.2	15.3±1.4	15.8±1.2	15.5±1.2	1.7±0.2
11g	42.0±1.6	2.6±0.4	17.6±1.2	14.1±1.1	39.4±1.6	0.1±0.9
11h	24.5±1.4	6.7±0.8	23.3±1.4	12.7±1.1	21.2±1.2	8.1±1.0
11i	20.5±1.3	7.7±0.9	18.2±1.3	10.5±1.0	5.9±0.8	37.3±1.5
11j	20.1±1.3	6.0±0.8	22.5±1.4	20.5±1.1	53.0±1.7	20.8±1.3
11k	18.2±1.5	12.7±1.3	10.5±1.1	18.3±1.3	20.4±1.3	8.6±0.7
11l	14.3±1.8	18.8±1.3	13.9±1.1	18.7±1.3	14.5±1.2	2.8±0.5

IC_{50} values were obtained from three independent repeats and represented as mean ± SD.

Among the 2-chalcone substituted derivatives tested, the compounds with electron donor substituents in the chalcone B-ring had a better antiproliferative activity than the compounds with the electron acceptor substituents. The compounds carrying a methoxy group on the chalcone B-ring displayed higher antiproliferative activities than compounds **7e**, **7f**, **7g**,**7h** carrying an electron-withdrawing chlorine atom. Compound **7d**, carrying no substituents on the B-ring, was inactive. This is consistent with Panchapakesan's studies[37].

The 16-benzylidene substituted 2-methoxyestradiol derivatives had moderate antiproliferative activity in six cancer cell lines tested. We found that 16-benzylidene-substituted estradiol derivatives with an electron-withdrawing halogen in the chalcone B-ring have enhanced the antiproliferative potential against the SMMC-7721 cells excluding **11d**. However, the only electron donor-substituted 16-benzylidene derivative **11l** containing 3,4,5-trimethoxy group had better antiproliferative activities.

Due to haemolysis induced by high concentrations of DMSO, we chose compounds **7b**, **7d**, **11b**, **11d**, **11e**, **11g**, **11h** and **11k** with high water solubility for further screening to investigate the antiangiogenic effects in the chick embryo chorioallantoic membrane model. The chicken embryo provides a unique model for investigating the blood vessel response to antiangiogenic agents. The control chicken chorioallantoic membranes showed well-developed neovascular zones under the filter saturated with carrier buffer after 3 days' culture, whereas the neovascularization in the chicken chorioallantoic membranes treated with **11b**, **11e**, **11g** and **11d** were significantly suppressed; however, **7b** and **7d** showed less significant difference. In addition, we evaluated the toxicity of these compounds against HEK-293 cells (human embryonic kidney cell line), the IC_{50} was assessed by MTT method and the results were shown in **Table 2**, these compounds showed low toxicity on normal cell line except **7b**.

The 16-benzylidene-modified 2-methoxyestradiol analog **11e** significantly reduced the number of blood vessels and vascular area resembling the antiangiogenic effect of

2ME2.

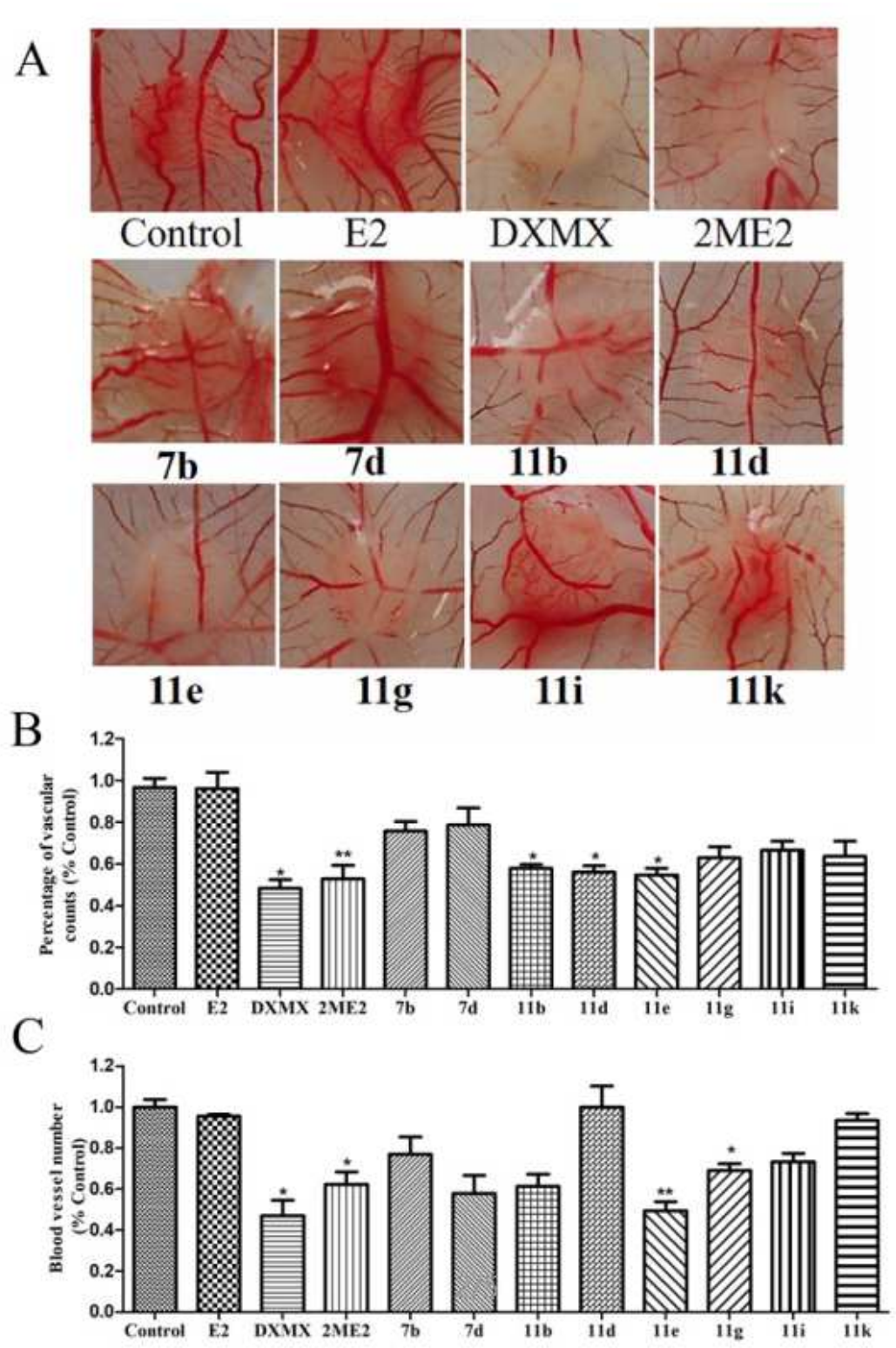

Fig 3 Screening compounds by chick chorioallantoic membrane assay. (A) Antiangiogenic activities of different drugs were measured using CAM assay. Control (normal saline 50 μg/mL), E2 (17β-estradiol 50 μg/mL), DXMX (dexamethasone 50 μg/mL), 2ME2 (50 μg/mL), and the compounds (50 μg/mL). Statistical analysis of percentage of the vascular counts (B) and the number of blood vessels (C). Data

are presented as the means ± SD, n=3, *p < 0.05 and **p < 0.01 versus Control.

Table 2 Cytotoxic activity against HEK-293 cells (IC_{50})

Compounds	**7b**	**7d**	**11b**	**11d**
IC_{50} (μM)	13.1±0.7	＞100	87.8±5.5	77.1±12.4
Compounds	**11e**	**11g**	**11i**	**11k**
IC_{50} (μM)	＞100	48.9±7.1	＞100	51.0±1.4

Compound 11e inhibits tumour growth in the human breast cancer (MCF-7) xenograft models

On basis of our results, we chose **11e** for further study due to its potent antiangiogenic and moderate cytotoxic activity in cancer cells. 2ME2 is an endogenous metabolite of estradiol that is regarded as a potential compound for the treatment of breast cancer, and the MCF-7 cell is a breast cancer cell line with strong angiogenesis and tumour growth abilities. Hence, the antitumour activities of 2ME2 and **11e** were examined in the nude mice subcutaneously implanted with the MCF-7 cells. The body weights and tumor volumes were measured and recorded every other day. As shown in **Fig 4B**, **C,** after 21-days' treatment, the tumour weights and tumour volumes were apparently decreased in the mice treated with **11e**. Meanwhile, the body weights of nude mice in control group and **11e** group gradually increased during the treatment period, while the body weights of nude mice in **2ME2** group significantly lower than that in the other groups, suggesting **11e** possessed a lower toxicity than 2ME2 (**Fig 5D**). The results indicated that **11e** may be a more effective and safer antitumour agent than 2ME2.

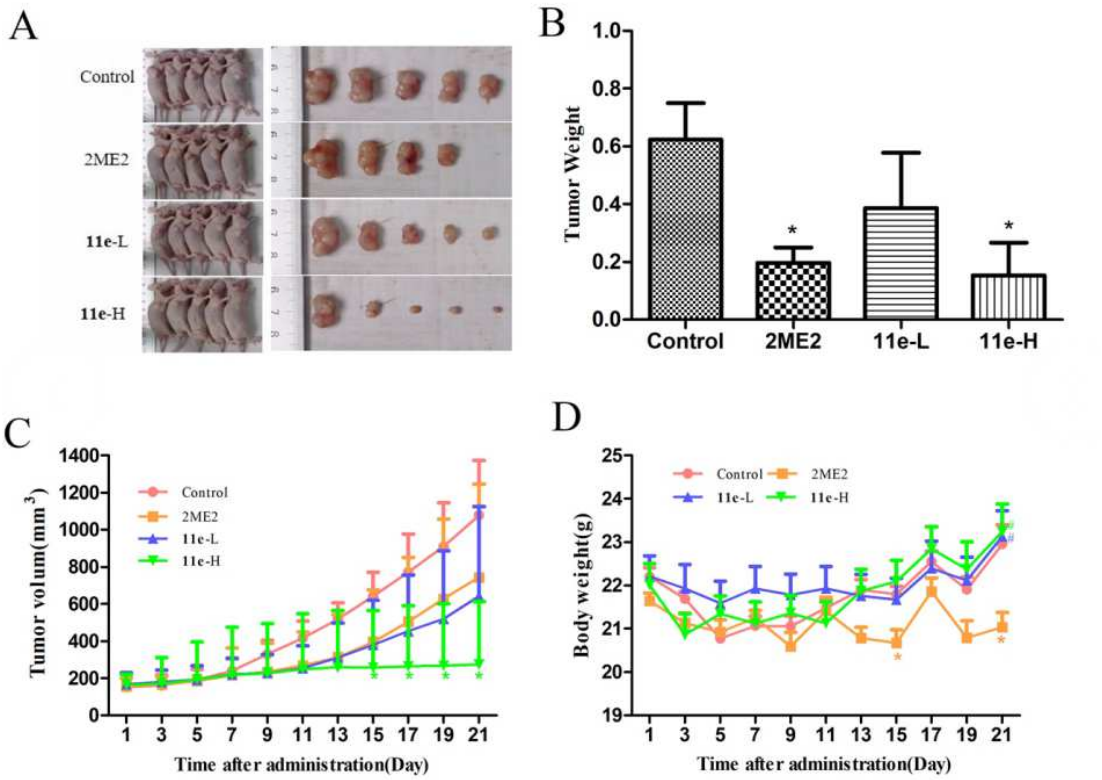

Fig 4 Compound **11e** inhibited the tumour growth *in vivo*. The nude mice were dosed by an intraperitoneal injection with Control (normal saline, 0.2 mL/day), 2ME2 (45 mg/kg/day), **11e**-L (22.5 mg/kg/day) and **11e**-H (45 mg/kg/day) for 21 days (n = 5 mice/group). (A) Nude mice and tumours at the end of therapy (day 21). (B) Tumour weight at the end of treatment (day 21). (C) Tumour volumes and (D) Body weights for the athymic nude mice during 21 days' treatment. Data are presented as the means ± SD, n=5/group. *$p < 0.05$ and **$p< 0.01$ versus Control group, $^{\#}p< 0.05$ versus 2ME2 group.

Toxicity evaluation of compound 11e *in vivo* and *in vitro*

To evaluate the toxicity of **11e**, we collected main organs including heart, liver, spleen, lung, and kidney in nude mice and used Hematoxylin and eosin staining (HE staining) to examine the tissue damage. As shown in **Fig 5A**, there was obvious liver cell edema in the 2ME2 group, while the **11e** group showed lower liver cell edema, other organs were not significantly affected. To further evaluate the liver damage, we examined the levels of the enzymes in the serum associated with the liver function including alanine transaminase (ALT), aspartate transaminase (AST) and alkaline phosphatase (ALP). As shown in **Fig 5B**, the levels of the three markers were increased in the 2ME2 group; however, the **11e** group had relatively small changes, the mean levels of the three enzymes of **11e** group were lower than that of 2ME2 group, indicating that **11e** is safer than 2ME2.

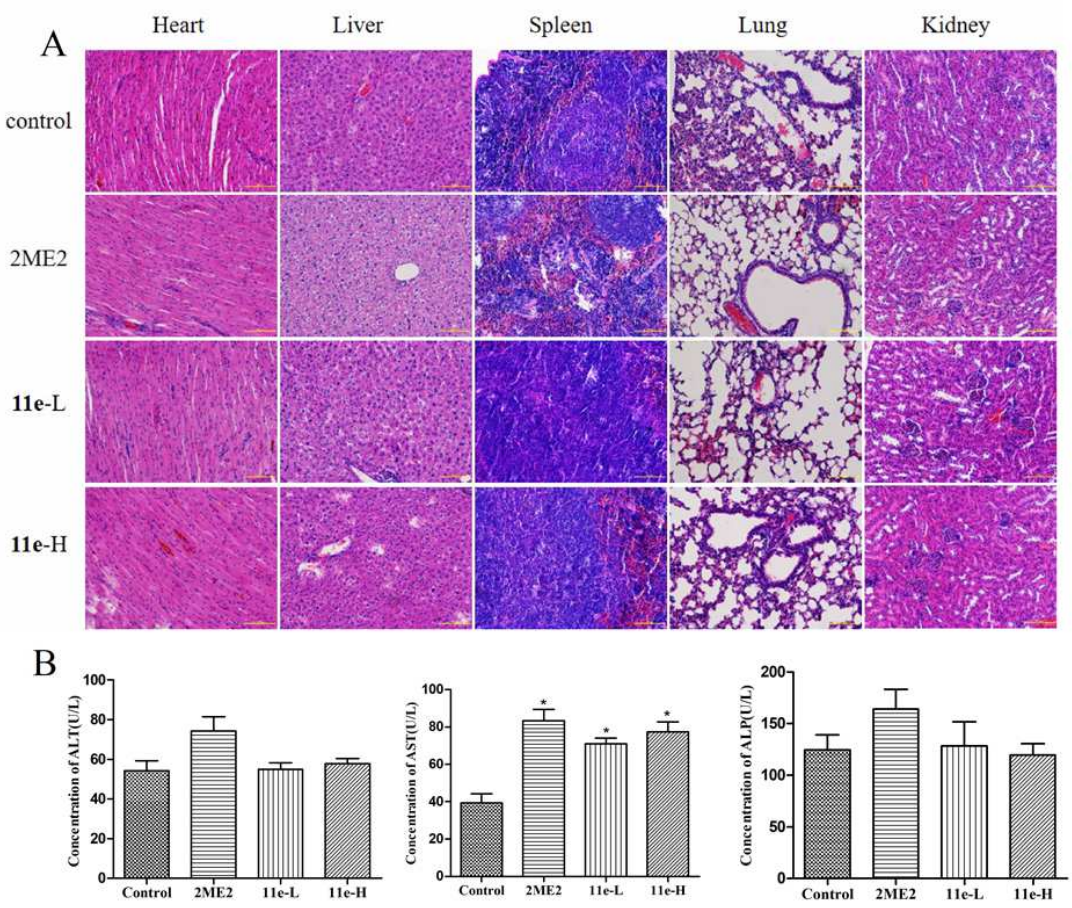

Fig 5 Histopathological examination and biochemical serum analysis in xenograft models. (A) HE staining for major organs (heart, liver, spleen, lung, kidney) in each group. The scale bars represent 100 μm. (B) Concentrations of ALT, AST and ALP in the serum of the mice. Control (normal saline, 0.2 mL/day), 2ME2 (45 mg/kg/day), **11e**-L (22.5 mg/kg/day) and **11e**-H (45 mg/kg/day) Data are presented as the mean ± SD. *p < 0.05 and **p < 0.01 versus Control group. $^{\#}$p<.0.05 versus 2ME2 group.

Additionally, we evaluated the cytotoxicity of **11e** and 2ME2 in normal human cells and in cancer cells, including HUVEC (human umbilical vein endothelial cells), GES-1 (human immortalized gastric epithelial cells), MCF-7 (breast cancer), MGC-803 (gastric cancer), PC-3 (prostate cancer). As shown in **Table 1**, the IC_{50} of **11e** is higher than that of 2ME2. As shown in **Fig 6**, cell viabilities were gradually reduced when given increasingly dose of 2ME2 and **11e** while at the same dose the cytotoxicity of **11e** was lower than that of 2ME2, indicating that the powerful effect of **11e** on inhibition of tumour growth is not dependent on a direct cytotoxicity effect.

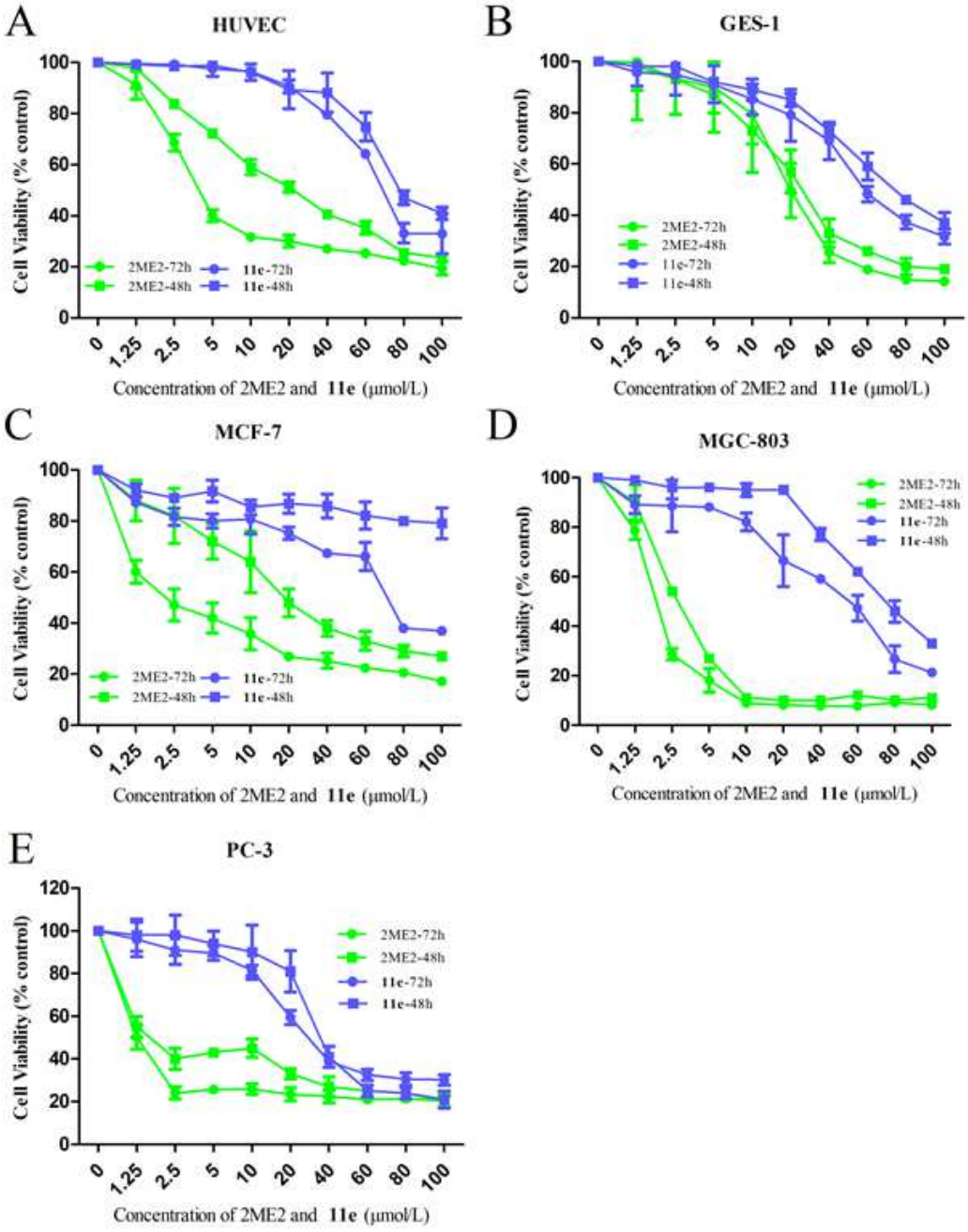

Fig 6 Compound **11e** had low cytotoxicity in normal and cancer cells. Cell viability curves were measured after **11e** or 2ME2 treatment for 48 h or 72 h in (A-E) HUVEC, GES-1, MCF-7, MGC-803, PC-3 cell lines respectively. Data are presented as the mean±SD of 3 independent tests.

Compound 11e inhibits the migration of HUVEC cells *in vitro*.

Compound **11e** inhibited the migration of HUVEC cells *in vitro*. Migration of human endothelial cells is prerequisite for angiogenesis. Thus, we evaluated whether **11e** could inhibit the migration of endothelial cells. HUVECs were treated with 0 μM (Control), 2 μM (low dose group) or 10 μM (high dose group) of **11e**, and the migration ability was

evaluated by the wound healing assay. The results showed that the migration rate of **11e** treatment group is lower than that of control group, which demonstrated **11e** could inhibit cell migration（**Fig.7A B**）. Similar results were observed in transwell assay(**Fig.7C D**).

The VEGF/VEGFR signaling pathway plays an important role in angiogenesis. Hence, we examined the expression of VEGFR. Western blotting analysis showed that **11e** reduced the expression of VEGFR in HUVECs. FAK is a protein tyrosine kinase associated with cell migration and the SHC adapter protein acts as a signal transporter in the regulation of endothelial cell migration. The expression of SHC and phosphorylated FAK was lower in **11e** treatment group while the total FAK levels were unchanged (**Fig.7E**, **F**). These data indicated that **11e** suppressed blood vessel formation which may relate to the reduction of VEGFR expression and phosphorylated FAK and SHC.

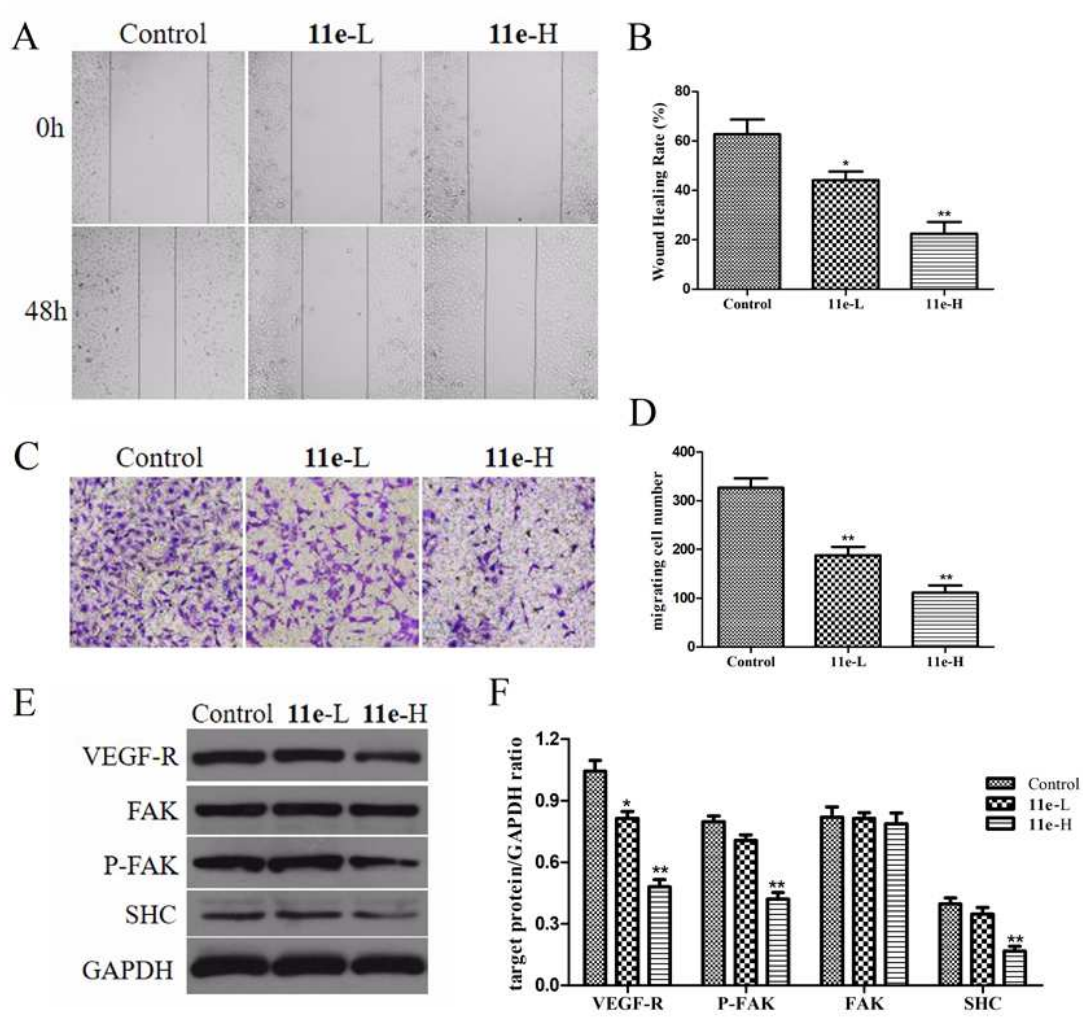

Fig 7 The effect and mechanism of **11e** on HUVEC cells migration *in vitro*. (A, B) Effect and statistical analysis of **11e** on HUVECs migration in wound healing assay. (C, D) Effect and statistical analysis of **11e** on HUVECs migration in transwell assay. (E, F) Expression and statistical analysis of VEGFR, FAK, P-FAK, SHC in HUVECs treated with different concentrations of **11e** for 48 h. Control: treated with no drug, **11e**-L: treated with 2 μM **11e**, **11e**-H: treated with 10 μM **11e**. All data are represented as

the mean ± SD of 3 independent tests. *p < 0.05 and **p < 0.01 versus Control.

Compound 11e inhibits the migration of MCF-7 cells *in vitro*.

The cell viability was tested, as is listed in Table 3, **11e** showed little toxicity both on breast cancer cells (MCF-7, MDA-MB-231), healthy human embryonic kidney cells (HEK-293) and human esophageal epithelial cells (Het-1A). Migration is characteristic for endothelial and cancer cells and is essential for angiogenesis and tumour metastasis. We evaluated whether **11e** can suppress migration in cancer cells. MCF-7 breast cancer cells were selected due to their high metastatic potential and the effect of **11e** on tumour cell migration was studied *in vitro* by wound healing assay. The **11e**-L (2 μM) and **11e**-H (10 μM) groups had lower wound healing rate of the MCF-7 cells compared with that in the control group (**Fig 8A-B**). As shown in **Fig 8C-D**, the transwell assay showed cell number from the upper chamber to the bottom chamber were reduced with the treatment of **11e**. Compared with the control group, compound **11e** significantly inhibited MCF-7 cell migration.

EMT plays an important role in the process of tumor invasion and metastasis. To elucidate the possible mechanism of inhibition on migration, we detected the expression of ZO-1, E-cadherin, N-cadherin, and Vimentin by the Western blotting assay. The results indicated that **11e** increased the expression of the epithelial marker proteins ZO-1 and E-cadherin and the expression of the mesenchymal markers N-cadherin and Vimentin were decreased, which indicated that **11e** can inhibit the EMT process in MCF-7 cells.

Table 3 Cytotoxic activity of 11e (IC_{50})

	MCF-7	MDA-MB-231	Het-1A	HEK-293
11e (μM)	77.0±2.7	78.6±8.3	＞100	＞100

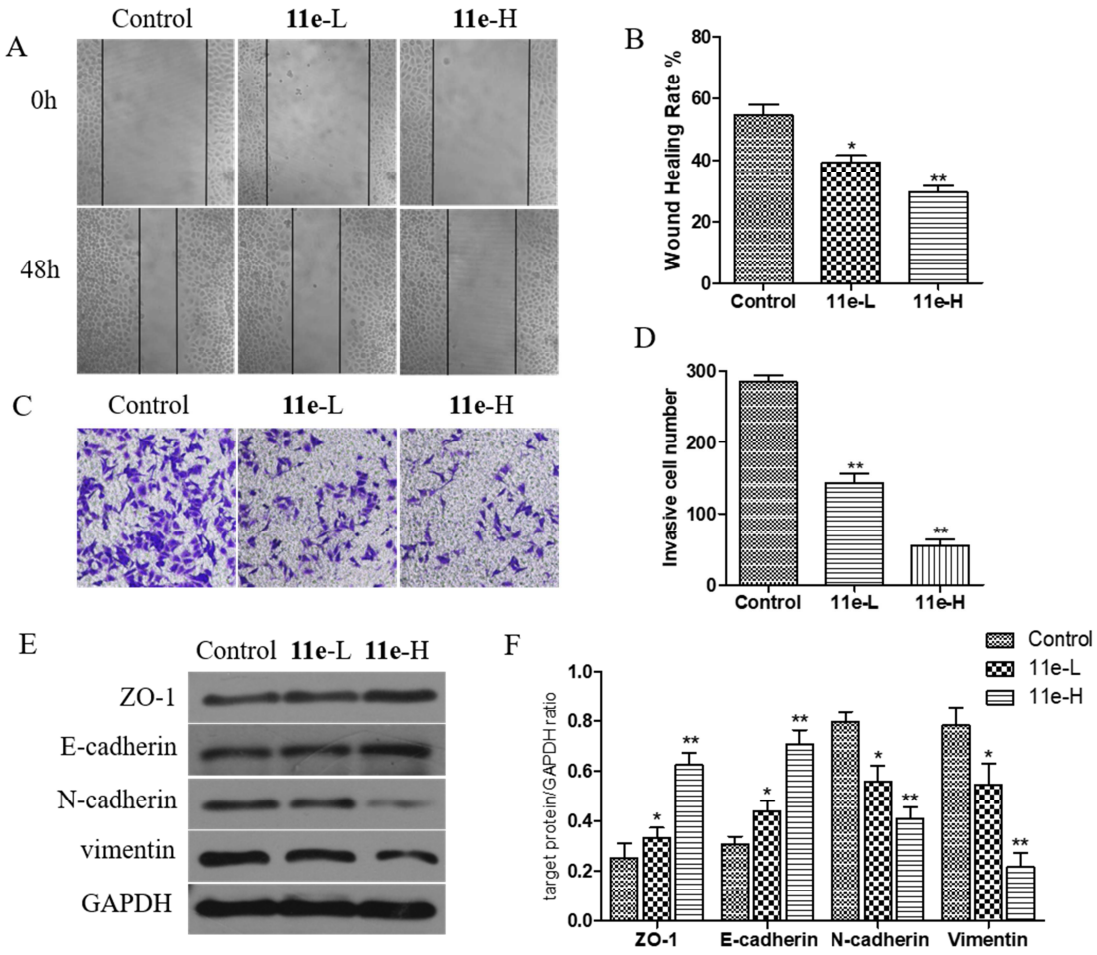

Fig 8 The effect and mechanism of **11e** on MCF-7 cells migration in vitro. (A, B) Effect and statistical analysis of **11e** on MCF-7 cell migration in wound healing assay. (C, D) Effect and statistical analysis of **11e** on MCF-7 cell migration in transwell assay. (E, F) Expression and statistical analysis of ZO-1, E-cadherin, N-cadherin and vimentin in MCF-7 cells treated with different concentrations of **11e** for 48 h. Control: treated with no drug, **11e**-L: treated with 2 μM **11e**, **11e**-H: treated with 10 μM **11e.** Data are represented as the means ± SD of 3 independent tests. *p < 0.05 and **p < 0.01 versus Control.

Discussion

Breast cancer is the most common cancer in women and is the leading cause of death among women[45]. Accumulating evidence indicates that the development of breast cancer is predominantly associated with increased lifetime exposure to endogenous and exogenous hormones[46]. 2ME2 is a potent antitumour and antiangiogenic compound for the treatment of breast cancer and prostate cancer[29, 47, 48]. Some progress has made for the treatment of breast cancer with 2ME2 structural modification, for example, isoform-specific sulfamate derivatives are responsible for the high specificity on Carbonic anhydrase IX (CA IX)[33], quinazolinone-modified 2-methoxyestradiol showed antiproliferative activity against breast cancer cells[49].

Here, we first synthesized chalconyl estradiol analogs and evaluated the

antiproliferative activity. The results showed chalconyl substituted derivatives played an insignificant cytotoxic effect on SKN-SH, B16, EC-109, MGC-803, A549, SMMC-7721 cell lines. And following, we evaluated the anti-angiogenic efficacy of these compounds using the chorioallantoic assay, the potent inhibition efficacy on angiogenesis of **11e** was observed. Our results showed that **11e** decreased the expression of VEGFR, the signal transporter SHC and thus downregulated the activation of FAK, these changes may associate with the inhibition efficacy on angiogenesis and cell migration of **11e**. **11e** had a similar efficacy as 2ME2 on angiogenesis while the antitumour effect of **11e** *in vivo* was superior to that of 2ME2 suggesting that **11e** had other anticancer targets. Then we tested the influence of **11e** on cell migration in MCF-7 cells, and the results showed that **11e** increased the epithelial marker proteins (ZO-1 and E-cadherin), while the mesenchymal markers proteins (N-cadherin and Vimentin) were decreased, which illustrated **11e** targets epithelial to mesenchymal transition (EMT).

EMT is the transition from an epithelial-like phenotype into a mesenchymal phenotype adopted early during metastatic progression to permit invasion and migration of the metastatic cells to secondary site within the body[50]. In carcinomas, the difference between cancer stem cells (CSCs) and non□CSCs is likely to be attributable largely to the cellular biological programme EMT[51, 52]. Activation of the EMT programme in the neoplastic cells was demonstrated to be closely associated with the CSC state revealing multifaceted effects of the EMT programme in driving the malignant phenotype of carcinoma cells[53, 54]. CSCs are a fundamental component of the metastatic cascade and will lead to novel therapeutic strategies against metastatic cancer[55-57]. In addition, CSCs are particularly adept in stimulating angiogenesis to promote tumour growth and to increase overall tumour aggressiveness before and after the therapy[58, 59], It is reported that CSCs generate proangiogenic factors to stimulate angiogenesis and at the same time, the tumour vasculature assists in maintenance of CSC self-renewal[60]. Our results showed that **11e** plays potent effects on angiogenesis and EMT, and because the two have close connection with CSCs, we speculate that **11e** may target CSCs and then exhibit a potent efficacy on antitumor. That is what we are searching for in the following study.

Conclusion

In this study, we synthesized a series of 2ME2 analogs containing the chalcone moiety that had antiangiogenic effects. **11e** was identified as the most potent derivate using the CAM assay. The growth of MCF-7 xenografted tumour *in vivo* was significantly inhibited by **11e** and there were less obvious adverse effects on major organs in nude mice. Further mechanistic studies indicated that the antiangiogenic effect of **11e** was mediated by inhibition of migration and downregulating of VEGFR expression in human endothelial cells. The migration of cancer cells was also suppressed by **11e** which may relate to the inhibition of EMT. Our preclinical results suggest that **11e** is a promising compound for the treatment of breast carcinoma.

Experimental section

General chemistry

All the chemicals and solvent were purchased from commercial sources. Solvents and reagents were dried and purified according to the methods described in the literature. Column chromatography was carried out using silica gel (200-300 mesh); analytical thin-layer chromatography (TLC) was performed on silica gel GF_{254} (Qingdao Haiyang Chemical Co, Ltd). ^{1}H and ^{13}C NMR spectra were recorded on a Bruker AVANCE DPX-400 NMR spectrometer (operating at 400 MHz for ^{1}H and 101 MHz for ^{13}C). The numbering used for assignment of the NMR signals is reported in supplement material. High resolution mass spectra (HRMS) were recorded on an Esquire 3000 mass spectrometer by electrospray ionization (ESI) after dissolving the compounds in methanol. Melting points were determined using a Beijing Keyi melting point apparatus XT5A and were uncorrected. Estradiol was purchased from Zhejiang Xianju Pharmaceutical Co., Ltd. All solvents were of analytical grade unless stated otherwise.

General procedure for the synthesis of compound

General procedure for the synthesis of 2-chalconyl substituted estradiol derivatives

We followed the method described by Rao et al. to prepare compounds **5** and **6**. Then 2-acetyl-estradiol-17β-acetate (**6**) reacted with corresponding aldehyde through the Claisen-Schmidt reaction to provide (*E*)-Estradiol-2-yl-3'-arylprop-2'-en-1'-one derivatives.

1. (2'*E*)-1-Estra-1,3,5(10)-trien-3,17β-dihydroxy-2yl-3'-arylprop-2'-en-1'-one

To a stirred solution of arylaldehyde (0.65 mmol) in 95% ethanol (10 mL), an aqueous solution of 10% NaOH (5 mL) was added, then 2-Acetyl-estradiol-17β-acetate **6** (0.2 g, 0.56 mmol) in 95% ethanol (5 mL) was slowly added. The reaction mixture was further stirred at 60 □ for 2 h. After completion, the reaction mixture was cooled to 0ºC and neutralized with 10% HCl aqueous solution. When the solution was adjusted to a pH ~ 5 (pH paper), an abundant yellow precipitate was formed. The precipitate was filtered and purified by chromatography (PE: EA=3:1) to give following compounds

1.1.

(2'*E*)-1-(3,17β-dihydroxy-1,3,5(10)-estratrienyl)-3'-(2"-methoxyphenyl)-prop-2'-en-1'-one (7a)

Yellow solid. 80% yield, mp. 155.6-156.6 □; ^{1}H NMR (400 MHz, $CDCl_3$) δ 12.69 (s, 1H, 3-OH), 8.19 (d, J = 15.7 Hz, 1H, 21-vinylic-H, CH=C-CO), 7.80 (s, 1H, 1-CH), 7.73 (d, J = 15.7 Hz, 1H, 20-vinylic-H, =CH-CO), 7.65 (dd, J = 7.7, 1.6 Hz, 1H, 27-CH), 7.44 – 7.36 (m, 1H, 25-CH), 7.02 (t, J = 7.8 Hz, 1H, 26-CH), 6.96 (d, J = 8.3 Hz, 1H, 24-CH), 6.73 (s, 1H, 4-CH), 3.93 (s, 3H, 23-OCH_3), 3.75 (t, J = 7.6 Hz, 1H, 17α-CH), 2.89 (ddd, J = 15.2, 7.4, 3.3 Hz, 2H, 6-CH_2), 2.43~1.17(m, 13H, rest of the 5×CH_2 and 3×CH of steroidal ring), 0.81 (s, 3H, 18-CH_3). ^{13}C NMR (101 MHz, $CDCl_3$) δ 194.0(CO), 161.2 (C23), 158.9 (C3), 147.0 (C5), 140.4 (C21), 132.0 (C27), 131.3 (C10), 129.4 (C25), 126.3 (C1), 123.8 (C22), 121.2 (C20), 120.8 (C26), 118.3 (C2), 117.7 (C24), 111.3 (C4), 81.8 (C17), 55.6 (OCH_3), 50.1 (C14), 43.6 (C9), 43.2 (C13), 38.6 (C8), 36.6 (C12), 30.6 (C16), 30.0 (C6), 26.9 (C7), 26.4 (C11), 23.1 (C15), 11.1 (C18). ES(-) (MeOH): (m/z) calculated for $C_{28}H_{31}O_4$([M-H]$^-$), 431.2228; found 431.2227.

1.2.

(2'*E*)-1-(3,17β-dihydroxy-1,3,5(10)-estratrienyl)-3'-(3"-methoxyphenyl)-prop-2'-en-1'-one (7b)

Yellow solid. 79% yield, mp. 189.6-191.6 □; ^{1}H NMR (400 MHz, $CDCl_3$) δ 12.59 (s, 1H, 3-OH), 7.85 (d, J = 15.5 Hz, 1H, 21-vinylic-H, CH=C-CO), 7.76 (s, 1H, 1-CH), 7.58 (d, J = 15.5 Hz, 1H, 20-vinylic-H, =CH-CO), 7.36 (t, J = 7.9 Hz, 1H, 26-CH), 7.27 (d, J = 7.8 Hz, 1H, 27-CH), 7.20 – 7.14 (m, 1H, 23-CH), 7.03 – 6.94 (m, 1H, 25-CH), 6.73 (s, 1H, 4-CH), 3.87 (s, 3H, 24-OCH_3), 3.75 (t, J = 8.5 Hz, 1H, 17α-CH), 2.87 (dd, J = 10.5, 4.8 Hz, 2H, 6-CH_2), 2.46~1.16(m, 13H, rest of the 5×CH_2 and 3×CH of steroidal ring), 0.81 (s, 3H, 18-CH_3). ^{13}C NMR (101 MHz, $CDCl_3$) δ 193.3 (CO), 161.3 (C24), 160.0 (C3), 147.4 (C5), 144.8 (C21), 136.2 (C22), 131.5 (C10), 130.0 (C26), 126.2 (C1), 121.1 (C27), 120.8 (C20), 118.1 (C2), 117.8 (C4), 116.0 (C25), 114.3 (C23), 81.8 (C17), 55.4 (OCH_3), 50.1 (C14), 43.6 (C9), 43.2 (C13), 38.6 (C8), 36.6 (C12), 30.6 (C16), 30.0 (C6), 26.8 (C7), 26.4 (C11), 23.1 (C15), 11.1 (C18). ES(-) (MeOH): (m/z) calculated for $C_{28}H_{31}O_4$([M-H]$^-$), 431.2228; found 431.2225.

1.3.

(2'*E*)-1-(3,17β-dihydroxy-1,3,5(10)-estratrienyl)-3'-(4"-methoxyphenyl)-prop-2'-en-1'-one（7c）

Yellow solid. 77% yield, mp. 213.5-214.9 ℃; ^{1}H NMR (400 MHz, $CDCl_3$) δ 12.72 (s, 1H, 3-OH), 7.88 (d, J = 15.4 Hz, 1H, 21-vinylic-H, CH=C-CO), 7.78 (s, 1H, 1-H), 7.64 (d, J = 8.8 Hz, 2H, 23- and 27-CH), 7.50 (d, J = 15.4 Hz, 1H, 20-vinylic-H, =CH-CO), 6.97 (t, J = 5.7 Hz, 2H, 24- and 26-CH), 6.73 (s, 1H, 4-CH), 3.87 (s, 3H, 25-OCH_3),

3.76 (t, J = 8.4 Hz, 1H, 17α-CH), 2.88 (dd, J = 10.5, 4.8 Hz, 2H, 6-CH_2), 2.46~1.16(m, 13H, rest of the 5×CH_2 and 3×CH of steroidal ring)), 0.81 (s, 3H, 18-CH_3). ^{13}C NMR (101 MHz, $CDCl_3$) δ 193.3(C19, CO), 161.9 (C25), 161.2(C3), 147.1 (C21), 144.8 (C5), 131.4 (C10), 130.5 (C23 and C27), 127.5 (C1), 126.0 (C22), 118.2 (C20), 117.9 (C2), 117.8 (C24 and C26), 114.5 (C4), 81.8 (C17), 55.5 (OCH_3), 50.1 (C14), 43.6 (C9), 43.2 (C13), 38.6 (C8), 36.6 (C12), 30.7 (C16), 30.0 (C6), 26.9 (C7), 26.4 (C11), 23.1 (C15), 11.1 (C18). ES(-) (MeOH): (m/z) calculated for $C_{28}H_{31}O_4$([M-H]$^-$), 431.2228; found 431.2226.

1.4.

(2'*E*)-1-(3,17β-dihydroxy-1,3,5(10)-estratrienyl)-3'-(4"-benzyloxyphenyl)-prop-2'-en-1'-one（7d）

Yellow solid. 75% yield, mp. 222.8-226.8 ℃; ^{1}H NMR (400 MHz, $CDCl_3$) δ 12.72 (s, 1H, 3-OH), 7.88 (d, J = 15.4 Hz, 1H, 21-vinylic-H, CH=C-CO), 7.78 (s, 1H, 1-CH), 7.63 (d, J = 8.7 Hz, 2H, 23- and 27-CH), 7.51 (d, J = 15.4 Hz, 1H, 20-vinylic-H, =CH-CO), 7.47~7.32(m, 5H, benzylic-5×CH), 7.04 (d, J = 8.8 Hz, 2H, 24- and 26-CH), 6.74 (s, 1H, 4-CH), 5.13 (s, 2H, benzylic-CH_2), 3.76 (t, J = 8.2 Hz, 1H,17α-CH), 2.88 (dd, J = 10.7, 4.7 Hz, 2H, 6-CH_2), 2.45~1.14(m, 13H, rest of the 5×CH_2 and 3×CH of steroidal ring), 0.81 (s, 3H, 18-CH_3). ^{13}C NMR (101 MHz, $CDCl_3$) δ 193.3 (CO), 161.2 (C3), 161.0(C25), 147.1 (C21), 144.7(C5), 136.4 (benzylic-C), 131.4 (C10), 130.5 (C23) and C27), 128.7 (benzylic-*m*-CH), 128.2 (benzylic-*p*-CH), 127.7 (benzylic-*o*-CH), 127.5 (C1), 126.1 (C22), 118.2 (C20), 118.0 (C2), 117.8 (C24 and C26), 115.4 (C4), 81.9 (C17), 70.2 (benzylic-CH_2), 50.1 (C14), 43.6 (C9), 43.2 (C13), 38.7 (C8), 36.6 (C12), 30.7 (C16), 30.0 (C6), 26.9 (C7), 26.5 (C11), 23.1 (C15), 11.1 (C18). ES(-) (MeOH): (m/z) calculated for $C_{34}H_{35}O_4$([M-H]$^-$), 507.2541; found 507.2539.

1.5.

(2'*E*)-1-(3,17β-dihydroxy-1,3,5(10)-estratrienyl)-3'-(2"-chlorophenyl)-prop-2'-en-1'-one（7e）

Yellow solid. 78% yield, mp. 166.0-168.2 ℃; ^{1}H NMR (400 MHz, $CDCl_3$) δ 12.49 (s, 1H, 3-OH), 8.26 (d, J = 15.6 Hz, 1H, 21-vinylic-H, CH=C-CO), 7.83 – 7.73 (m, 2H, 1- and 24-CH), 7.58 (d, J = 15.6 Hz, 1H, 20-vinylic-H, =CH-CO), 7.50 – 7.43 (m, 1H, 27-CH), 7.40 – 7.32 (m, 2H, 25- and 26-CH), 6.75 (s, 1H, 4-CH), 3.75 (t, J = 8.5 Hz, 1H, 17α-CH), 2.88 (dd, J = 9.4, 6.3 Hz, 2H, 6-CH2), 2.44~1.14(m, 13H, rest of the 5×CH_2 and 3×CH of steroidal ring), 0.80 (s, 3H, 18-CH_3). ^{13}C NMR (101 MHz, $CDCl_3$) δ 193.2 (CO), 161.3 (C3), 147.6 (C21), 140.6 (C5), 135.6 (C10), 133.2 (C23), 131.6 (C22), 131.4 (C24), 130.4 (C25), 128.0 (C1), 127.1 (C27) ,126.3 (C26), 123.2 (C20), 118.0 (C2), 117.9 (C4), 81.8 (C17), 50.01 (C14), 43.6 (C9), 43.2 (C13), 38.6 (C8), 36.6 (C12), 30.6 (C16), 30.0 (C6), 26.8 (C7), 26.4 (C11), 23.1 (C15), 11.1 (C18). ES(-) (MeOH): (m/z) calculated for $C_{27}H_{28}ClO_3$([M-H]$^-$), 435.1732; found 435.1730.

1.6.

(2'*E*)-1-(3,17β-dihydroxy-1,3,5(10)-estratrienyl)-3'-(3"-chlorophenyl)-prop-2'-en-1'-one（7f）

Yellow solid. 80% yield, mp. 161.0-162.3 ℃; ^{1}H NMR (400 MHz, $CDCl_3$) δ 12.52 (s, 1H, 3-OH), 7.80 (d, J = 15.5 Hz, 1H, 21-vinylic-H, CH=C-CO), 7.74 (s, 1H, 1-CH), 7.63 (s, 1H, 23-CH), 7.58 (d, J = 15.5 Hz, 1H, 20-vinylic-H, =CH-CO), 7.52 (d, J = 6.6 Hz, 1H, 27-CH)), 7.44 – 7.34 (m, 2H, 25- and 26-CH)), 6.74 (s, 1H, 4-CH), 3.76 (t, J = 8.5 Hz, 1H, 17α-CH), 2.96 – 2.81 (m, 2H, 6-CH_2), 2.48~1.19(m, 13H, rest of the 5×CH_2 and 3×CH of steroidal ring), 0.81 (s, 3H, 18-CH_3). ^{13}C NMR (101 MHz, $CDCl_3$) δ 193.0 (CO), 161.3 (C3), 147.7 (C21), 143.2 (C5), 136.6 (C22), 135.0 (C10), 131.7 (C24), 130.5 (C26), 130.3 (C1), 128.1 (C25), 126.9 (C27), 126.1 (C23), 121.7 (C20), 118.0 (C2), 117.9 (C4), 81.8 (C17), 50.1 (C14), 43.6 (C9), 43.2 (C13), 38.6 (C8), 36.6 (C12), 30.6 (C16), 30.1 (C6), 26.8 (C7), 26.5 (C11), 23.1 (C15), 11.1 (C18). ES(-) (MeOH): (m/z) calculated for $C_{27}H_{28}ClO_3$([M-H]$^-$), 435.1732; found 435.1731.

1.7.

(2'*E*)-1-(3,17β-dihydroxy-1,3,5(10)-estratrienyl)-3'-(4"-chlorophenyl)-prop-2'-en-1'-one（7g）

Yellow solid. 79% yield, mp. 206.8-210.0 ℃; ^{1}H NMR (400 MHz, $CDCl_3$) δ 12.55 (s, 1H, 3-OH), 7.83 (d, J = 15.5 Hz, 1H, 21-vinylic-H, CH=C-CO), 7.75 (s, 1H, 1-CH), 7.58 (dd, J = 12.0, 7.1 Hz, 3H, 20- vinyl-H, 23- and 27-CH), 7.41 (d, J = 8.5 Hz, 2H, 24- and 26-CH), 6.74 (s, 1H, 4-CH), 3.76 (t, J = 8.5 Hz, 1H, 17α-CH), 2.94 – 2.83 (m, 2H, 6-CH_2), 2.45~1.15(m, 13H, rest of the 5×CH_2 and 3×CH of steroidal ring), 0.81 (s, 3H, 18-CH_3). ^{13}C NMR (101 MHz, $CDCl_3$) δ 193.0 (CO), 161.3 (C3), 147.6 (C21), 143.4 (C5), 136.7 (C10), 133.3 (C25), 131.6 (C22), 129.8 (C23 and C27), 129.3 (C24 and C26), 126.1 (C1), 120.8 (C20), 118.1 (C2), 117.9 (C4), 81.8 (C17), 50.1 (C14), 43.6 (C9), 43.2 (C13), 38.6 (C8), 36.6 (C12), 30.6 (C16), 30.0 (C6), 26.8 (C7), 26.4 (C11), 23.1 (C15), 11.1 (C18). ES(-) (MeOH): (m/z) calculated for $C_{27}H_{28}ClO_3$([M-H]$^-$), 435.1732; found 435.1730.

1.8.

(2'*E*)-1-(3,17β-dihydroxy-1,3,5(10)-estratrienyl)-3'-(2",4"-bichlorophenyl)-prop-2'-en-1'-one（7h）

Yellow solid. 81% yield, mp. 206.8-210.0 ℃; ^{1}H NMR (400 MHz, $CDCl_3$) δ 12.43 (s, 1H, 3-OH), 8.18 (d, J = 15.5 Hz, 1H, 21-vinylic-H, CH=C-CO), 7.73 (s, 1H, 1-CH), 7.70 (d, J = 8.5 Hz, 1H, 24-CH), 7.56 (d, J = 15.5 Hz, 1H, 20-vinylic-H, =CH-CO), 7.49 (d, J = 2.1 Hz, 1H, 27-CH), 7.33 (dd, J = 8.4, 2.0 Hz, 1H, 26-CH), 6.75 (s, 1H, 4-CH), 3.75 (dd, J = 12.8, 8.3 Hz, 1H, 17α-CH), 2.89 (dd, J = 9.5, 6.3 Hz, 2H, 6-CH2), 2.42~1.14(m, 13H, rest of the 5×CH_2 and 3×CH of steroidal ring) , 0.80 (s, 3H, 18-CH_3). ^{13}C NMR (101 MHz, $CDCl_3$) δ 192.9 (CO), 161.3 (C3), 147.8 (C21), 139.3

(C5), 136.7 (C23), 136.2 (C10), 131.8 (C22), 131.7 (C27), 130.2 (C24), 128.7 (C1), 127.6 (C26), 126.2 (C25), 123.5 (C20), 118.0 (C2), 117.9 (C4), 81.8 (C17), 50.1 (C14), 43.6 (C9), 43.2 (C13), 38.6 (C8), 36.6 (C12), 30.6 (C16), 30.0 (C6), 26.8 (C7), 26.4 (C11), 23.1 (C15), 11.1 (C18). ES(-) (MeOH): (m/z) calculated for $C_{27}H_{27}Cl_2O_3$([M-H]$^-$), 469.1343; found 469.1340.

General procedure for the synthesis of 11a~k

We followed the method described by Rao et al. to get compound **8**, **9**, and **10**. Then 2-methoxy-3-acetyloxyestrone (**9**) or 2-methoxyestrone (**10**) react with corresponding aldehyde through the Claisen-Schmidt reaction to provide16*E*-benzylidene 2-methoxyestrone derivatives.

2. (*E*)-16-(arylidene)-3-hydroxy-2-methoxy-estra-1,3,5(10) trien-17-one (11)

To a stirred solution of **10** (0.2 g, 0.67 mmol) [or 9(0.23 g, 0.67 mmol)] in ethanol (20 mL), was added an aqueous solution of 10% KOH (2 mL), then corresponding benzaldehyde (7.50 mmol, 1.5 equiv) was added. The reaction mixture was stirred for 3 h in the room temperature and then poured into cold water. When the resulting solution was neutralized with 10% HCl aqueous solution, a lot of yellow precipitation formed. The precipitates were filtered under reduced pressure, washed with water, dried and crystallized from methanol to obtain compound **11a~k.**

2.1. (*E*)-16-(benzylidene)-3-hydroxy-2-methoxy-estra-1,3,5(10) trien-17-one (11a)

Yellow solid. yield 91%. mp. 202.5-206.4 □; ^{1}H NMR (400 MHz, $CDCl_3$) δ 7.56 (d, J = 7.4 Hz, 2H, 22 and 26-CH), 7.48 (s, 1H, 16-arylidene-CH), 7.43 (t, J = 7.3 Hz, 2H, 23 and 25-CH), 7.40–7.34 (m, 1H, 24-CH), 6.80 (s, 1H, 4-CH), 6.67 (s, 1H, 1-CH), 5.52 (s, 1H, 3-OH), 3.87 (s, 3H, 2-OCH_3), 2.99 (dd, J = 15.7, 5.6 Hz, 1H, 15b-CH), 2.92–2.79 (m, 2H, 6-CH_2), 2.60–2.49 (m, 1H, 15a-CH), 2.46–1.39 (m, 9H, rest of the 3×CH_2 and 3×CH of steroidal ring), 1.01 (s, 3H, 18-CH_3). ^{13}C NMR (101 MHz, $CDCl_3$) δ 209.7 (CO), 144.8 (C2), 143.7 (C3), 136.0 (C16), 135.6 (C20), 133.3 (C10), 131.2 (C21), 130.4 (C5), 129.3 (C22 and C26), 129.2 (C23 and C25), 128.7 (C24), 114.7 (C4), 108.0 (C1), 56.1 (OCH_3), 48.6 (C14), 47.9 (C13), 44.4 (C9), 38.0 (C8), 31.8 (C12), 29.1 (C6), 28.9 (C7), 26.9 (C11), 26.3 (C15), 14.6(C18). ES(-) (MeOH): (m/z) calculated for $C_{26}H_{27}O_3$([M-H]$^-$), 387.1966; found 387.1965.

2.2. (*E*)-16-(4'-flurobenzylidene)-3-hydroxy-2-methoxy-estra-1,3,5(10) trien-17-one (11b)

Light yellow solid. yield 93%. mp. 231.2-233.5 □; ^{1}H NMR (400 MHz, $CDCl_3$) δ 7.55 (dd, J = 8.0, 5.7 Hz, 2H, 22 and 26-CH), 7.44 (s, 1H, 16-arylidene-CH), 7.12 (t, J = 8.5 Hz, 2H, 23 and 25-CH), 6.80 (s, 1H, 4-CH), 6.67 (s, 1H, 1-CH), 5.49 (s, 1H,

3-OH), 3.88 (s, 3H, 2-OCH_3), 2.95 (dd, J = 15.6, 6.4 Hz, 1H, 15b-CH), 2.92–2.81 (m, 2H, 6-CH_2), 2.51 (t, J = 14.1 Hz, 1H, 15a-CH), 2.47 -1.39 (m, 9H, rest of the 3×CH_2 and 3×CH of steroidal ring), 1.01 (s, 3H, 18-CH_3). ^{13}C NMR (101 MHz, $CDCl_3$) δ 209.5 (CO), 164.3 (C24), 144.8 (C2), 143.7 (C3), 135.6 (C16), 132.2 (C20), 132.2 (C10), 132.1(C21), 131.8 (C5), 131.2 (C22), 129.2 (C26), 116.0 (C23) , 115.8 (C25), 114.7 (C4), 108.0 (C1), 56.1 (OCH_3), 48.6 (C14), 47.8 (C13), 44.4 (C9), 38.0 (C8), 31.7 (C12), 29.0 (C6), 28.8 (C7), 26.9 (C11), 26.3 (C15), 14.6 (C18). ES(-) (MeOH): (m/z) calculated for $C_{26}H_{26}FO_3$([M-H]$^-$), 405.1871; found 405.1867.

2.3. (*E*)-16-(3',5'-difluorobenzylidene)-3-hydroxy-2-methoxy-estra-1,3,5(10) trien-17-one (11c)

Yellow solid. yield 95%. mp. 234.1-237.6 □; ^{1}H NMR (400 MHz, $CDCl_3$) δ 7.42–7.37 (m, 1H, 26-CH), 7.36 (d, J = 1.9 Hz, 1H, 16-arylidene-CH), 7.29 (dd, J = 8.4, 4.2 Hz, 1H, 25-CH), 7.21 (dt, J = 9.7, 8.2 Hz, 1H, 22-CH), 6.80 (s, 1H, 4-CH), 6.68 (s, 1H, 1-CH), 5.47 (s, 1H, 3-OH), 3.87 (s, 3H, 2-OCH_3), 2.94 (ddd, J = 15.7, 6.4, 1.5 Hz, 1H, 15b-CH), 2.90-2.79 (m, 2H, 6-CH_2), 2.51 (ddd, J = 15.6, 12.7, 2.9 Hz, 1H, 15a-CH), 2.45-1.38(m, 9H, rest of the 3×CH_2 and 3×CH of steroidal ring), 1.00 (s, 3H, 18-CH_3). ^{13}C NMR (101 MHz, $CDCl_3$) δ 209.2 (CO), 144.7 (C23), 143.7 (C24), 136.8 (C2), 132.8 (C3), 131.0 (C16), 131.0 (C20), 129.2 (C10), 127.0 (C21), 118.6 (C5), 118.4 (C26), 117.8 (C25), 117.6 (C22), 114.7 (C4), 107.9 (C1), 56.1 (OCH3), 48.4 (C14), 47.9 (C13), 44.3 (C9), 37.9 (C8), 31.7 (C12), 28.9 (C6), 28.8 (C7), 26.9 (C11), 26.2 (C15), 14.6 (C18). ES(-) (MeOH): (m/z) calculated for $C_{26}H_{25}F_2O3$([M-H]$^-$), 423.1777; found 423.1775.

2.4. (*E*)-16-(3'-chlorobenzylidene)-3-hydroxy-2-methoxy-estra-1,3,5(10) trien-17-one (11d)

Light yellow solid. yield 93%. mp. 212.7-216.0 □; ^{1}H NMR (400 MHz, $CDCl_3$) δ 7.53 (s, 1H, 16-arylidene-CH), 7.45–7.41 (m, 1H, 26-CH), 7.39 (m, 1H, 25-CH), 7.37–7.32 (m, 2H, 22 and 24-CH), 6.80 (s, 1H, 4-CH), 6.68 (s, 1H, 1-CH)), 5.45 (s, 1H, 3-OH), 3.87 (s, 3H, 2-OCH_3), 2.96 (ddd, J = 15.9, 6.4, 1.6 Hz, 1H, 15b-CH), 2.91 – 2.79 (m, 2H, 6-CH), 2.54 (ddd, J = 15.7, 12.6, 3.0 Hz, 1H, 15a-CH), 2.47 –1.40(m, 9H, rest of the 3×CH_2 and 3×CH of steroidal ring), 1.01 (s, 3H, 18-CH_3). ^{13}C NMR (101 MHz, $CDCl_3$) δ 209.2 (CO), 144.8 (C2), 143.7 (C3), 137.4 (C16), 134.7 (C20 and C21), 131.7 (C10), 131.1 (C23), 129.9 (C5 and C25), 129.8 (C22), 129.2 (C24), 128.5 (C26), 114.7 (C4), 108.0 (C1), 56.1 (OCH3), 48.5 (C14), 47.9 (C13), 44.4 (C9), 38.0 (C8), 31.7 (C12), 29.0 (C6), 28.8 (C7), 26.9 (C11), 26.3 (C15), 14.6 (C18). ES(-) (MeOH): (m/z) calculated for $C_{26}H_{26}ClO_3$([M-H]$^-$), 421.1576; found 421.1576.

2.5. (*E*)-16-(4'-chlorobenzylidene)-3-hydroxy-2-methoxy-estra-1,3,5(10) trien-17-one (11e)

Light yellow solid. yield 92%. mp. 226.8-230.4 □; ^{1}H NMR (400 MHz, $CDCl_3$) δ

7.49 (d, J = 8.5 Hz, 2H, 22 and 26-CH), 7.45-7.40 (m, 2H, 23 and 25-CH), 7.38 (s, 1H, 16-arylidene-CH), 6.80 (s, 1H, 4-CH), 6.67 (s, 1H, 1-CH), 5.49 (s, 1H, 3-OH), 3.87 (s, 3H, 2-OCH_3), 2.94 (ddd, J = 15.7, 6.3, 1.5 Hz, 1H, 15b-CH), 2.86 (dd, J = 11.3, 5.7 Hz, 2H, 6-CH_2), 2.52 (ddd, J = 15.6, 12.6, 2.9 Hz, 1H, 15a-CH), 2.43 -1.40 (m, 9H, rest of the 3×CH_2 and 3×CH of steroidal ring) 1.01 (s, 3H, 18-CH3). ^{13}C NMR (101 MHz, $CDCl_3$) δ 209.4 (CO), 144.8 (C2), 143.7 (C3), 136.5 (C16), 135.2 (C20), 134.1 (C10), 131.9 (C24), 131.5 (C21), 131.1 (C25), 129.2 (C22 and C26), 129.0 (C23 and C25), 114.7 (C4), 108.0 (C1), 56.1 (OCH3), 48.5 (C14), 47.9 (C13), 44.4 (C9), 38.0 (C8), 31.7 (C12), 29.1 (C6), 28.8 (C7), 26.9 (C11), 26.3 (C15), 14.6 (C18). ES(-) (MeOH): (m/z) calculated for $C_{26}H_{26}ClO_3$([M-H]$^-$), 421.1576; found 421.1575.

2.6. (*E*)-16-(2',4'-dichlorobenzylidene)-3-hydroxy-2-methoxy-estra-1,3,5(10) trien-17-one (11f)

Yellow solid. yield 95%. mp. 225.1-228.7 □; ^{1}H NMR (400 MHz, $CDCl_3$) δ 7.73 (s, 1H, 23-CH), 7.50 (d, J = 8.4 Hz, 1H, 26-CH), 7.47 (s, 1H, 16-arylidene-CH), 7.29 (d, J = 8.2 Hz, 1H, 25-CH), 6.80 (s, 1H, 4-CH), 6.66 (s, 1H, 1-CH), 5.49 (s, 1H, 3-OH), 3.87 (s, 3H, 2-OCH_3), 2.99–2.71 (m, 3H, 15b-CH and 6-$CH_{2)}$, 2.49 (t, J = 14.0 Hz, 1H, 15a-CH), 2.42-1.36 (m, 9H, rest of the 3×CH2 and 3×CH of steroidal ring), 1.02 (s, 3H, 18-CH_3). ^{13}C NMR (101 MHz, $CDCl_3$) δ 208.6 (CO), 144.8 (C2), 143.7 (C3), 138.7 (C16), 136.4 (C22), 135.3 (C20), 132.4 (C10), 131.0 (C21), 130.5 (C26), 129.9 (C5), 129.2 (C23), 128.3 (C25), 127.0 (C24), 114.7 (C4), 108.0 (C1), 56.1 (OCH_3), 48.5 (C14), 48.1 (C13), 44.3 (C9), 37.9 (C8), 31.7 (C12), 28.9 (C6), 28.8 (C7), 26.9 (C11), 26.2 (C15), 14.5 (C18). ES(-) (MeOH): (m/z) calculated for $C_{26}H_{25}Cl_2O_3$([M-H]$^-$), 455.1186; found 455.1186.

2.7. (*E*)-16-(4'-bromobenzylidene)-3-hydroxy-2-methoxy-estra-1,3,5(10) trien-17-one (11g)

Light yellow solid. yield 92%. mp. 246.5-249.0 □; ^{1}H NMR (400 MHz, $CDCl_3$) δ 7.55 (d, J = 8.5 Hz, 2H, 22 and 26-CH), 7.43 (s, 1H, 16-arylidene-CH), 7.42-7.38 (m, 2H, 23 and 25-CH), 6.80 (s, 1H, 4-CH), 6.67 (s, 1H, 1-CH), 5.50 (s, 1H, 3-OH), 3.87 (s, 3H, 2-$OCH_{3)}$, 2.93 (ddd, J = 15.7, 6.4, 1.5 Hz, 1H, 15b-CH), 2.86 (dd, J = 11.4, 5.6 Hz, 2H, 6-CH_2), 2.50 (ddd, J = 15.7, 12.6, 3.0 Hz, 1H, 15a-CH), 2.46-1.42 (m, 9H, rest of the 3×CH_2 and 3×CH of steroidal ring), 1.00 (s, 3H, 18-CH_3). ^{13}C NMR (101 MHz, $CDCl_3$) δ 209.3 (CO), 144.8 (C2), 143.7 (C3), 136.7 (C16), 134.5 (C20 and C10), 132.0 (C21), 131.7 (C23 and C25), 131.1 (C22 and C26), 129.2 (C5), 123.5 (C24), 114.7 (C4), 108.0 (C1), 56.1 (OCH_3), 48.5 (C14), 47.9 (C13), 44.3 (C9), 38.0 (C8), 31.7 (C12), 29.1 (C6), 28.8 (C7), 26.9 (C11), 26.3 (C15), 14.6 (C18). ES(-) (MeOH): (m/z) calculated for $C_{26}H_{26}ClO_3$([M-H]$^-$), 465.1071; found 465.1072.

2.8. (*E*)-16-(3'-nitrobenzylidene)-3-hydroxy-2-methoxy-estra-1,3,5(10) trien-17-one (11h)

Light yellow solid. yield 94%. mp. 234.1-238.5 □; ^{1}H NMR (400 MHz, CDCl3) δ 8.41 (s, 1H, 22-CH), 8.22 (d, J = 8.0 Hz, 1H, 24-CH), 7.84 (d, J = 7.5 Hz, 1H, 26-CH), 7.61 (t, J = 8.0 Hz, 1H, 25-CH), 7.49 (s, 1H, 16-arylidene-CH), 6.80 (s, 1H, 4-CH), 6.68 (s, 1H, 1-CH), 5.49 (s, 1H, 3-OH), 3.88 (s, 3H, 2-$OCH_{3)}$, 2.99 (dd, J = 15.8, 6.2 Hz, 1H, 15b-CH), 2.95-2.82 (m, 2H, 6-CH_2), 2.62 (t, J = 13.5 Hz, 1H, 15a-CH), 2.48-1.40 (m, 9H, rest of the 3×CH_2 and 3×CH of steroidal ring), 1.03 (s, 3H, 18-CH_3). ^{13}C NMR (101 MHz, $CDCl_3$) δ 208.8 (CO), 148.5 (C23), 144.8 (C2), 143.8 (C3), 138.9 (C16), 137.3 (C21), 136.0 (C20), 130.9 (C10), 130.4 (C26), 129.7 (C5), 129.2 (C25), 124.2 (C24), 123.6 (C22), 114.7 (C4), 108.0 (C1), 56.1 (OCH3), 48.4 (C14), 48.0 (C13), 44.4 (C9), 37.9 (C8), 31.7 (C12), 29.0 (C6), 28.8 (C7), 26.9 (C11), 26.2 (C15), 14.5 (C18). ES(-) (MeOH): (m/z) calculated for $C_{26}H_{27}NO_5$([M-H]$^-$), 433.1889; found 433.1887.

2.9. (*E*)-16-(4'-methylsulfonylbenzylidene)-3-hydroxy-2-methoxy-estra-1,3,5(10) trien-17-one (11i)

Light yellow solid. yield 93%. mp. 235.4-237.3 □; ^{1}H NMR (400 MHz, $CDCl_3$) δ 7.99 (d, J = 8.1 Hz, 2H, 22 and 26-CH), 7.72 (d, J = 8.2 Hz, 2H, 23 and 25-CH), 7.48 (s, 1H, 16-arylidene-CH), 6.80 (s, 1H, 4-CH), 6.67 (s, 1H, 1-CH), 5.50 (s, 1H, 3-OH), 3.87 (s, 3H, 2-OCH_3), 3.09 (s, 3H, 24-SO_2CH_3), 2.97 (dd, J = 15.9, 5.9 Hz, 1H, 15b-CH), 2.91-2.80 (m, 2H, 6-CH_2), 2.59 (t, J = 14.3 Hz, 1H, 15a-CH), 2.48 -1.40 (m, 9H, rest of the 3×CH_2 and 3×CH of steroidal ring), 1.03 (s, 3H, 18-CH_3). ^{13}C NMR (101 MHz, $CDCl_3$) δ 208.85 (CO), 144.8 (C2), 143.8 (C3), 141.0 (C16), 140.4 (C24), 139.6 (C20), 130.9 (C10), 130.7 (C21 and C25), 129.1 (C23 and C25), 127.7 (C22 and C26), 114.7 (C4), 108.0 (C1), 56.1 (OCH3), 48.4 (C14), 48.0 (C13), 44.5 (SO_2CH_3), 44.3 (C9), 38.0 (C8), 31.7 (C12), 29.2 (C6), 28.8 (C7), 26.9 (C11), 26.2 (C15), 14.5 (C18). ES(-) (MeOH): (m/z) calculated for $C_{27}H_{29}O_5S$([M-H]$^-$), 465.1741; found 465.1740.

2.10. (*E*)-16-(4'-methylbenzylidene)-3-hydroxy-2-methoxy-estra-1,3,5(10) trien-17-one (11j)

Light yellow solid. Yield: 89%. mp. 251.2-253.7 □; ^{1}H NMR (400 MHz, $CDCl_3$) δ 7.48 (s, 1H , 16-arylidene-CH), 7.46 (s, 2H, 22 and 26-CH), 7.23 (d, J = 7.9 Hz, 2H, 23 and 25-CH), 6.80 (s, 1H, 4-CH), 6.67 (s, 1H, 1-CH), 5.48 (s, 1H, 3-OH), 3.87 (s, 3H, 2-OCH_3), 2.98 (dd, J = 15.6, 5.2 Hz, 1H, 15b-CH), 2.85 (dt, J = 17.0, 8.3 Hz, 2H, 6-CH2), 2.60-2.51 (m, 1H, 15a-CH), 2.39 (s, 3H, 24-CH_3), 2.49 -1.39 (m, 9H, rest of the 3×CH_2 and 3×CH of steroidal ring)1.00 (s, 3H, 18-CH_3). ^{13}C NMR (101 MHz, $CDCl_3$) δ 209.7 (CO), 144.8 (C2), 143.7 (C3), 139.7 (C16), 135.1 (C24), 133.3 (C20), 132.9 (C10), 131.3 (C21), 130.4 (C5), 129.5 (C23 and C25), 129.3 (C22 and C26), 114.7 (C4), 108.0 (C1), 56.1 (OCH_3), 48.7 (C14), 47.8 (C13), 44.4(C9), 38.0(C8), 31.8(C12), 29.2(C6), 28.9(C7), 26.9(C11), 26.3 (C15), 21.5 (24-CH_3), 14.6 (C18). ES(-)

(MeOH): (m/z) calculated for $C_{27}H_{29}O_3$([M-H]$^-$), 401.2122; found 401.2122.

2.11. (*E*)-16-(2',3'-dimethoxy benzylidene)-3-hydroxy-2-methoxy-estra-1,3,5(10) trien-17-one (11k)

Yellow solid. Yield: 89%. mp. 185.2-188.6 □; ^{1}H NMR (400 MHz, $CDCl_3$) δ 7.81 (s, 1H, 16-arylidene-CH), 7.16 (d, J = 7.2 Hz, 1H, 26-CH), 7.10 (t, J = 8.0 Hz, 1H, 25-CH), 6.95 (d, J = 7.3 Hz, 1H, 24-CH), 6.80 (s, 1H, 4-CH), 6.66 (s, 1H, 1-CH), 5.49 (s, 1H, 3-OH), 3.89 (s, 3H, 22-OCH_3), 3.87 (s, 3H, 2-OCH_3), 3.85 (s, 3H, 23-OCH_3), 2.89 (dd, J = 15.3, 7.1 Hz, 1H, 15b-CH), 2.85–2.77 (m, 2H, 6-CH_2), 2.50 (ddd, J = 15.7, 12.8, 3.0 Hz, 1H, 15a-CH), 2.43-1.36(m, 9H, rest of the 3×CH_2 and 3×CH of steroidal ring), 1.01 (s, 3H, 18-CH_3). ^{13}C NMR (101 MHz, $CDCl_3$) δ 209.5 (CO), 153.0 (C22), 149.1 (C23), 144.7 (C2), 143.7 (C3), 137.1 (C16), 131.3 (C20), 129.9 (C10), 129.3 (C5), 128.0 (C25), 123.7 (C26), 121.4 (C21), 114.7 (C24), 113.4 (C4), 108.0 (C1), 61.4 (OCH3), 56.1 (OCH_3), 55.9 (OCH_3), 48.5 (C14), 47.9 (C13), 44.3 (C9), 38.0 (C8), 31.8 (C12), 29.2 (C6), 28.9 (C7), 26.9 (C11), 26.3 (C15), 14.6 (C18). ES(-) (MeOH): (m/z) calculated for $C_{28}H_{31}O_5$([M-H]$^-$), 447.2177; found 447.2176.

2.12. (*E*)-16-(3',4',5'-trimethoxybenzylidene)-3-hydroxy-2-methoxy-estra-1,3,5(10) trien-17-one (11l)

Yellow solid. Yield: 82%. mp. 191-198 □; ^{1}H NMR (400 MHz, $CDCl_3$) δ 7.40 (s, 1H, 16-arylidene-CH), 6.81 (s, 3H, 4, 22 and 26-CH), 6.67 (s, 1H, 1-CH), 5.48 (s, 1H, 3-OH), 3.91 (s, 6H, 23 and 25-OCH_3), 3.90 (s, 3H, 24-OCH_3), 3.87 (s, 3H, 2-OCH_3), 3.07-2.94 (m, 1H, 15b-CH), 2.86 (m, 2H, 6-CH), 2.52 (ddd, J = 15.4, 12.6, 2.8 Hz, 1H, 15a-H), 2.46-1.40 (m, 9H, rest of the 3×CH_2 and 3×CH of steroidal ring), 1.01 (s, 3H, 18-CH_3). ^{13}C NMR (101 MHz, $CDCl_3$) δ 209.5 (CO), 153.3 (C23 and C25), 144.8 (C2), 143.7 (C3), 139.5 (C16), 135.1 (C24), 133.5 (C20), 131.1 (C10), 129.2 (C5), 114.7 (C22 and C26), 108.0 (C4), 107.8 (C1), 61.0 (OCH_3), 56.3 (OCH_3), 56.1 (OCH_3), 48.6 (C14), 47.8 (C13), 44.4 (C9), 37.9 (C8), 31.8 (C12), 28.9 (C6), 28.8 (C7). 26.9 (C11), 26.3 (C15), 14.6 (C18). ES(-) (MeOH): (m/z) calculated for $C_{29}H_{33}O_6$([M-H]$^-$), 477.2283; found 477.2284.

Cell line and cell culture

The human breast cancer cell line MCF-7 was purchased from Chinese Academy of Sciences, and the human umbilical vein endothelial cells (HUVECs) were purchased from Jiangsu KeyGEN Biotechology Corporation. All cells were cultured in RPMI 1640 medium supplemented with 10% fetal bovine serum (FBS), 100 units/mL penicillin, and 100 μg/mL streptomycin. The cells were incubated in a humidified atmosphere of 5% CO_2 at 37 ˚C.

Cytotoxicity assay *in vitro*

SRB assay

Cytotoxic activity was evaluated by colorimetric sulforhodamine B (SRB) assay. Briefly, cancer cells in the exponential growth phase were treated with trypsin and diluted to 5×10^4 cells/mL. Then, 100 μL of the cell suspension was transferred into 96 well plates. After cells were cultured overnight, the synthesized derivatives were added at indicated concentrations and the results were compared with the control group. After treatment for 72 h, the cells were fixed with 10% TCA for 1 h, stained with SRB for 15 min, and dissovled with Tris-HCl. The absorbance of each hole in the 96 well plates was measured by a Multiskan Spectrum reader. The concentration causing 50% cell growth inhibition (IC_{50}) was calculated and analyzed by the SPSS 15.0 software.

MTT assay

Cytotoxicity was determined by the MTT assay. Briefly, the cells were seeded in 96-well plates at a density of 3×10^3 cells per well and incubated overnight. Then, the cells were changed to fresh medium containing various concentrations of drugs. After 48 h or 72 h, 20 μL MTT was added to each well at a final concentration of 500 μg/mL and cells were incubated for 4 h. Then, the precipitate was completely dissolved by 150 μL of DMSO and the absorbance was measured at 570 nm.

Chick chorioallantoic membrane (CAM) assay

Inhibition effect of angiogenesis *in vivo* was measured using CAM assay. Briefly, fertilized chicken eggs were incubated at 37˚C for 6 days. Then, a small hole was punched in the broad side of an egg and a window was carefully created through the eggshell. The CAM of the embryo was treated with E2, 2ME2, DXMX and compounds we synthesized. The eggs were returned to a humidified egg incubator and chicken chorioallantoic membranes were fixed and harvested after 72h. Angiogenesis was quantified by counting the number of blood vessel numbers and imaged the neovascularization zones. Ten eggs were used per group to ensure the reproducibility of the assay.

Wound healing assay

Cells were seeded in 6-well plates and then scraped off in each well using a sterile 100 μL pipette tip. Subsequently, cells were washed twice to remove detached cells. Then, cells were incubated in medium containing 2% FBS. The wound gaps were imaged using a microscope connected to a digital camera and then drugs were added. After 48 h incubation, the wound gaps were once again imaged and the migration rates were examined.

Transwell assay

Cells were seeded on the top side of the polycarbonate transwell filters in the serum-free medium. The complete serum-containing medium was used as a chemoattractant in the bottom chamber. After 24 h, migrated cells were fixed in 4% paraformaldehyde for 20 min, stained with crystal violet for 20 min, and imaged by a Nikon fluorescence microscope.

Western blotting

Cells were lysed by RIPA lysis buffer containing 1% protease and phosphatase inhibitor cocktail on ice for 30 min. The lysates were then centrifuged at 12,000 g for 10 min at 4 ºC and supernatant were collected. The total protein concentrations were determined by a BCA Kit. The proteins were added with proper loading buffer and boiled to denature. These proteins were resolved by 8% SDS-PAGE and transferred to polyinylidene difluoride membranes. After blocking the nonspecific binding sites with 5% non-fat milk, the membranes were incubated with primary antibodies overnight at 4 ˚C and then incubated with the secondary antibodies for 2 h at room temperature. The protein bands were visualized by an enhanced chemiluminescence (ECL) detection system. The densitometric analysis were performed using Image J software.

Animals and tumour xenograft model

All animal experiments were conducted in accordance with the ethical standards and have been approved by the Ethics Committee of Zhengzhou University. Male/Female nude mice (aged 4-6 week, perchased from Silikejingda, Hunan) were raised in individually ventilated cages and received adequate sterile water and food. For the xenograft models, MCF-7 cells (5×10^7 in 200 μL saline) were subcutaneously injected into the right forelimb of nude mice. When the average tumour volume reached 100mm^3, the animals were randomized and assigned to the following groups: control (nomal saline, 0.2 mL/day), 2ME2 (45 mg/kg/day), **11e**-L (22.5 mg/kg/day) and **11e**-H (45 mg/kg/day) (n=5 mice/group); corresponding drugs were dosed by an intraperitoneal injection to each group and lasted 21 days. Body weights and tumour volumes were measured every other day. Tumour volume was calculated using the following formula: tumour volume (mm^3) = length ×width ×width/2. 21 days' treatment, the nude mice were killed and major organs were collected, fixed in 4% buffered paraformaldehyde and paraffin-embedded for hematoxylin and eosin (HE) staining for toxicity assessment.

Biochemical serum analysis

Toxicity and adverse effects were observed by assessing animal body weight, hepatic serum marker and damage to major organs. Blood samples were collected. Let the

samples sit at room temperature for 30 min, and centrifuge the blood sample at 4000 rpm for 4 min, collect the supernatant which is serum. According to the instructions to prepare the relevant solution and add it into the sample bottle of the automatic biochemical analyzer, set the relevant procedures to start the determination for biochemical serum analysis of alkaline phosphatase (ALP), alanine transaminase (ALT), and aspartate transaminase (AST).

Histological analysis

Hematoxylin and eosin (HE) staining was used to assess cell necrosis. Major organs (heart, liver, spleen, lung and kidney) were collected, fixed in 4% buffered paraformaldehyde and paraffin-embedded for HE staining. We prepared 5 μm tumour sections from paraffin-embedded tumour tissue samples. The sections were deparaffinized in xylene, rehydrated in ethanol, rinsed in distilled water, and then fixed with 4% formaldehyde. After fixed with formaldehyde, sections were stained with hematoxylin and eosin followed by dehydration in graded alcohol. The sections were mounted on glass slides previously treated with poly-L-Lysine and imaged using a microscope.

Statistical analysis

All experiments were repeated three times independently. Statistical analysis was performed using One-Way ANOVA for *in vitro* assay, and individual differences between the treatments were analyzed using the unpaired t-test by the Graphpad Prism software (All groups were compared in pairs). All comparisons are made relative to the untreated controls and significance of difference is indicated as $*p < 0.05$ and $**p < 0.01$.

Acknowledgments

This work was supported by the Science and Technology Research Key Project in the Henan province Department of Education (Project No. 18A350013 for Cong Wang). Project supported by the Henan foundation and frontier technology research program. the National Natural Foundation of China (Grant No. 81573364), the Science and technology key project of Henan province (No. 172102310171), and Zhengzhou University graduate student independent innovation project. Science and Technology Innovation Talents of Henan Provincial Education Department (19IRTSTHN001, by W.Z).

Abbreviation

MTT, 3-(4,5-dimethylthiazol-2-yl)-2,5-diphenyltetrazolium bromide;
SRB, sulforhodamine B;
2ME2, 2-methoxyestradiol;
VEGFR, Vascular Endothelial Growth Factor Receptor;
FAK, Focal Adhesion Kinase;
ZO-1, zonula occludens proteins;
ALP, alkaline phosphatase;
ALT, alanine transaminase;
AST, aspartate transaminase;
HE, hematoxylinand eosin staining;
RIPA, Radio-Immunoprecipitation Assay;
SDS-PAGE, Sodium Dodecane Sulonate -Polyacrylamide Gel Electrophoresis;
BCA, bicinchoninic acid;
DXMX, Dexamethasone;
CAM, Chick chorioallantoic membrane assay;
PBS, Phosphatidylserine;
DMSO, Dimethyl sulfoxide;
FBS, Fetal Bovine Serum;
HUVEC, Human Umbilical Vein Endothelial Cells;

References

[1] J. Folkman, Tumor angiogenesis: therapeutic implications, The New England journal of medicine 285(21) (1971) 1182-6.
[2] D. Hanahan, J. Folkman, Patterns and emerging mechanisms of the angiogenic switch during tumorigenesis, Cell 86(3) (1996) 353-64.
[3] D. Hanahan, R.A. Weinberg, Hallmarks of cancer: the next generation, Cell 144(5) (2011) 646-674.
[4] P. Carmeliet, R.K. Jain, Molecular mechanisms and clinical applications of angiogenesis, Nature 473(7347) (2011) 298-307.
[5] M. Potente, H. Gerhardt, P. Carmeliet, Basic and therapeutic aspects of angiogenesis, Cell 146(6) (2011) 873-87.
[6] S. Rey, L. Schito, B.G. Wouters, S. Eliasof, R.S. Kerbel, Targeting hypoxia-inducible factors for antiangiogenic cancer therapy, Trends in cancer 3(7) (2017) 529-541.
[7] S. Rey, G.L. Semenza, Hypoxia-inducible factor-1-dependent mechanisms of vascularization and vascular remodelling, Cardiovascular research 86(2) (2010) 236-42.

[8] A.F. List, Vascular endothelial growth factor signaling pathway as an emerging target in hematologic malignancies, Oncologist 6 (2001) 24-31.
[9] P. Baluk, H. Hashizume, D.M. McDonald, Cellular abnormalities of blood vessels as targets in cancer, Current opinion in genetics & development 15(1) (2005) 102-11.
[10] M. De Palma, D. Biziato, T.V. Petrova, Microenvironmental regulation of tumour angiogenesis, Nature reviews. Cancer 17(8) (2017) 457-474.
[11] P. Saharinen, L. Eklund, K. Pulkki, P. Bono, K. Alitalo, VEGF and angiopoietin signaling in tumor angiogenesis and metastasis, Trends in molecular medicine 17(7) (2011) 347-62.
[12] V. Baeriswyl, G. Christofori, The angiogenic switch in carcinogenesis, Seminars in cancer biology 19(5) (2009) 329-37.
[13] M. Graupera, M. Potente, Regulation of angiogenesis by PI3K signaling networks, Experimental cell research 319(9) (2013) 1348-55.
[14] Y.N. Shi, N. Zhu, C. Liu, H.T. Wu, Y. Gui, D.F. Liao, L. Qin, Wnt5a and its signaling pathway in angiogenesis, Clinica chimica acta; international journal of clinical chemistry 471 (2017) 263-269.
[15] G.G. Yue, B.C. Chan, H.F. Kwok, Y.L. Wong, H.W. Leung, C.J. Ji, K.P. Fung, P.C. Leung, N.H. Tan, C.B. Lau, Anti-angiogenesis and immunomodulatory activities of an anti-tumor sesquiterpene bigelovin isolated from inula helianthus-aquatica, European journal of medicinal chemistry 59 (2013) 243-52.
[16] W. Chen, G. Zhang, L. Guo, W. Fan, Q. Ma, X. Zhang, R. Du, R. Cao, Synthesis and biological evaluation of novel alkyl diamine linked bivalent beta-carbolines as angiogenesis inhibitors, European journal of medicinal chemistry 124 (2016) 249-261.
[17] A. Markowska, S. Sajdak, J. Markowska, A. Huczynski, Angiogenesis and cancer stem cells: new perspectives on therapy of ovarian cancer, European journal of medicinal chemistry 142 (2017) 87-94.
[18] L. Varella, J. Abraham, M. Kruse, Revisiting the role of bevacizumab in the treatment of breast cancer, Seminars in oncology 44(4) (2017) 273-285.
[19] J. Wang, L. Zhang, X. Pan, B. Dai, Y. Sun, C. Li, J. Zhang, Discovery of multi-target receptor tyrosine kinase inhibitors as novel anti-angiogenesis agents, Scientific reports 7 (2017) 45145.
[20] R.N. Gacche, R.J. Meshram, Angiogenic factors as potential drug target: Efficacy and limitations of anti-angiogenic therapy, Bba-Rev Cancer 1846(1) (2014) 161-179.
[21] A. Villanueva, D.Y. Chiang, P. Newell, J. Peix, S. Thung, C. Alsinet, V. Tovar, S. Roayaie, B. Minguez, M. Sole, C. Battiston, S. Van Laarhoven, M.I. Fiel, A. Di Feo, Y. Hoshida, S. Yea, S. Toffanin, A. Ramos, J.A. Martignetti, V. Mazzaferro, J. Bruix, S. Waxman, M. Schwartz, M. Meyerson, S.L. Friedman, J.M. Llovet, Pivotal role of mTOR signaling in hepatocellular carcinoma, Gastroenterology 135(6) (2008) 1972-83, 1983 e1-11.
[22] F. Fan, A. Schimming, D. Jaeger, K. Podar, Targeting the tumor microenvironment: focus on angiogenesis, Journal of oncology 2012 (2012) 281261.
[23] S. Frandsen, S. Kopp, M. Wehland, J. Pietsch, M. Infanger, D. Grimm, Latest results for anti-angiogenic drugs in cancer treatment, Current pharmaceutical design 22(39) (2016) 5927-5942.

[24] X. Shi, Z. Wang, F. Xu, X. Lu, H. Yao, D. Wu, S. Sun, R. Nie, S. Gao, P. Li, L. Xia, Z. Zhang, C. Wang, Design, synthesis and antiproliferative effect of 17β-amide derivatives of 2-methoxyestradiol and their studies on pharmacokinetics, Steroids 128 (2017) 6-14.
[25] B.S. Kumar, D.S. Raghuvanshi, M. Hasanain, S. Alam, J. Sarkar, K. Mitra, F. Khan, A.S. Negi, Recent Advances in chemistry and pharmacology of 2-methoxyestradiol: An anticancer investigational drug, Steroids 110 (2016) 9-34.
[26] D. Matei, J. Schilder, G. Sutton, S. Perkins, T. Breen, C. Quon, C. Sidor, Activity of 2 methoxyestradiol (Panzem (R) NCD) in advanced, platinum-resistant ovarian cancer and primary peritoneal carcinomatosis: A Hoosier Oncology Group trial, Gynecologic oncology 115(1) (2009) 90-96.
[27] S.V. Rajkumar, P.G. Richardson, M.Q. Lacy, A. Dispenzieri, P.R. Greipp, T.E. Witzig, R. Schlossman, C.F. Sidor, K.C. Anderson, M.A. Gertz, Novel therapy with 2-methoxyestradiol for the treatment of relapsed and plateau phase multiple myeloma, Clinical Cancer Research 13(20) (2007) 6162-6167.
[28] J. James, D.J. Murry, A.M. Treston, A.M. Storniolo, G.W. Sledge, C. Sidor, K.D. Miller, Phase I safety, pharmacokinetic and pharmacodynamic studies of 2-methoxyestradiol alone or in combination with docetaxel in patients with locally recurrent or metastatic breast cancer, Investigational new drugs 25(1) (2007) 41-48.
[29] N.J. Lakhani, M.A. Sarkar, J. Venitz, W.D. Figg, 2-Methoxyestradiol, a promising anticancer agent, Pharmacotherapy 23(2) (2003) 165-172.
[30] Q. Zhou, D. Gustafson, S. Nallapareddy, S. Diab, S. Leong, K. Lewis, L. Gore, W.A. Messersmith, A.M. Treston, S.G. Eckhardt, C. Sidor, D.R. Camidge, A phase I dose-escalation, safety and pharmacokinetic study of the 2-methoxyestradiol analog ENMD-1198 administered orally to patients with advanced cancer, Investigational new drugs 29(2) (2011) 340-346.
[31] J.M. Day, P.A. Foster, H.J. Tutill, S.P. Newman, Y.T. Ho, M.P. Leese, B.V. Potter, M.J. Reed, A. Purohit, BCRP expression does not result in resistance to STX140 in vivo, despite the increased expression of BCRP in A2780 cells in vitro after long-term STX140 exposure, British journal of cancer 100(3) (2009) 476-86.
[32] M.P. Thomas, B.V. Potter, Discovery and development of the aryl O-sulfamate pharmacophore for oncology and women's health, Journal of medicinal chemistry 58(19) (2015) 7634-58.
[33] J.T. Andring, W. Dohle, C. Tu, B.V.L. Potter, R. McKenna, 3,17β-Bis-sulfamoyloxy-2-methoxyestra-1,3,5(10)-triene and nonsteroidal sulfamate derivatives inhibit carbonic anhydrase IX: structure-activity optimization for isoform selectivity, Journal of medicinal chemistry 62(4) (2019) 2202-2212.
[34] S. Yousuf, M. Duan, E.L. Moen, S. Cross-Knorr, K. Brilliant, B. Bonavida, T. LaValle, K.C. Yeung, F. Al-Mulla, E. Chin, D. Chatterjee, Raf kinase inhibitor protein (RKIP) blocks signal transducer and activator of transcription 3 (STAT3) activation in breast and prostate cancer, Plos One 9(3) (2014) e92478.
[35] H. Mirzaei, M. Shokrzadeh, M. Modanloo, A. Ziar, G.H. Riazi, S. Emami, New indole-based chalconoids as tubulin-targeting antiproliferative agents, Bioorganic chemistry 75 (2017) 86-98.

[36] V. Brito, A.O. Santos, P. Almeida, S. Silvestre, Novel 4-azaandrostenes as prostate cancer cell growth inhibitors: Synthesis, antiproliferative effects, and molecular docking studies, Comptes Rendus Chimie 22(1) (2019) 73-83.
[37] G. Panchapakesan, V. Dhayalan, N. Dhatchana Moorthy, N. Saranya, A.K. Mohanakrishnan, Synthesis of 2-substituted 17β-hydroxy/17-methylene estratrienes and their in vitro cytotoxicity in human cancer cell cultures, Steroids 76(13) (2011) 1491-504.
[38] R. Bansal, P.C. Acharya, Synthesis and antileukemic activity of 16*E*-[4-(2-carboxy)ethoxybenzylidene]-androstene amides, Steroids 77(5) (2012) 552-7.
[39] A.M. Scherbakov, I.V. Zavarzin, S.K. Vorontsova, A. Hajra, O.E. Andreeva, A.V. Yadykov, I.S. Levina, Y.A. Volkova, V.Z. Shirinian, Synthesis and evaluation of the antiproliferative activity of benzylidenes of 16-dehydroprogesterone series, Steroids 138 (2018) 91-101.
[40] A. Berenyi, R. Minorics, Z. Ivanyi, I. Ocsovszki, E. Ducza, H. Thole, J. Messinger, J. Wolfling, G. Motyan, E. Mernyak, E. Frank, G. Schneider, I. Zupko, Synthesis and investigation of the anticancer effects of estrone-16-oxime ethers in vitro, Steroids 78(1) (2013) 69-78.
[41] H.O. Saxena, U. Faridi, J.K. Kumar, S. Luqman, M.R. Darokar, K. Shanker, C.S. Chanotiya, M.M. Gupta, A.S. Negi, Synthesis of chalcone derivatives on steroidal framework and their anticancer activities, Steroids 72(13) (2007) 892-900.
[42] P.N. Rao, J.W. Cessac, A new, practical synthesis of 2-methoxyestradiols, Steroids 67(13-14) (2002) 1065-70.
[43] R. Abonia, D. Insuasty, J. Castillo, B. Insuasty, J. Quiroga, M. Nogueras, J. Cobo, Synthesis of novel quinoline-2-one based chalcones of potential anti-tumor activity, European journal of medicinal chemistry 57 (2012) 29-40.
[44] A. Arenas-Gonzalez, L.A. Mendez-Delgado, P. Merino-Montiel, J.M. Padron, S. Montiel-Smith, J.L. Vega-Baez, S. Meza-Reyes, Synthesis of monomeric and dimeric steroids containing [1,2,4]triazolo[1,5-a]pyrimidines, Steroids 116 (2016) 13-19.
[45] R.L. Siegel, K.D. Miller, A. Jemal, Cancer statistics, 2018, CA: a cancer journal for clinicians 68(1) (2018) 7-30.
[46] M. Ellingjord-Dale, L. Vos, S. Tretli, S. Hofvind, I. Dos-Santos-Silva, G. Ursin, Parity, Hormones and breast cancer subtypes - results from a large nested case-control study in a national screening program, Breast Cancer Res 19(1) (2017) 10.
[47] J.F. Peyrat, J.D. Brion, M. Alami, Synthetic 2-methoxyestradiol derivatives: structure-activity relationships, Current medicinal chemistry 19(24) (2012) 4142-4156.
[48] A.O. Mueck, H. Seeger, 2-Methoxyestradiol--biology and mechanism of action, Steroids 75(10) (2010) 625-31.
[49] W. Dohle, F.L. Jourdan, G. Menchon, A.E. Prota, P.A. Foster, P. Mannion, E. Hamel, M.P. Thomas, P.G. Kasprzyk, E. Ferrandis, M.O. Steinmetz, M.P. Leese, B.V.L. Potter, Quinazolinone-based anticancer agents: synthesis, antiproliferative SAR, antitubulin activity, and tubulin Co-crystal structure, Journal of medicinal chemistry 61(3) (2018) 1031-1044.
[50] M.W. Klymkowsky, P. Savagner, Epithelial-mesenchymal transition: a cancer

researcher's conceptual friend and foe, The American journal of pathology 174(5) (2009) 1588-93.
[51] K. Polyak, R.A. Weinberg, Transitions between epithelial and mesenchymal states: acquisition of malignant and stem cell traits, Nature reviews. Cancer 9(4) (2009) 265-73.
[52] M.J. Wu, Y.S. Chen, M.R. Kim, C.C. Chang, S. Gampala, Y. Zhang, Y. Wang, C.Y. Chang, J.Y. Yang, C.J. Chang, Epithelial-mesenchymal transition directs stem cell polarity via regulation of mitofusin, Cell metabolism (2018).
[53] C. Scheel, R.A. Weinberg, Cancer stem cells and epithelial-mesenchymal transition: concepts and molecular links, Seminars in cancer biology 22(5-6) (2012) 396-403.
[54] S. Ansieau, EMT in breast cancer stem cell generation, Cancer letters 338(1) (2013) 63-8.
[55] F. Li, B. Tiede, J. Massague, Y. Kang, Beyond tumorigenesis: cancer stem cells in metastasis, Cell research 17(1) (2007) 3-14.
[56] G. Ahmad, M.M. Amiji, Cancer stem cell-targeted therapeutics and delivery strategies, Expert opinion on drug delivery 14(8) (2017) 997-1008.
[57] S. Li, Q. Li, Cancer stem cells, lymphangiogenesis, and lymphatic metastasis, Cancer letters 357(2) (2015) 438-47.
[58] C.E. Eyler, J.N. Rich, Survival of the fittest: cancer stem cells in therapeutic resistance and angiogenesis, Journal of clinical oncology: official journal of the American Society of Clinical Oncology 26(17) (2008) 2839-45.
[59] A.Z. Ayob, T.S. Ramasamy, Cancer stem cells as key drivers of tumour progression, Journal of biomedical science 25(1) (2018) 20.
[60] A.M. Mercurio, VEGF/Neuropilin signaling in cancer stem cells, International journal of molecular sciences 20(3) (2019).

Highlights

- 2-Methoxyestradiol (2ME2) has been considered as a potential antitumour agent mainly targeting angiogenesis.
- A novel class of chalcone modified 2ME2 compounds was first synthesized, and the *E*-conformation in the α,β-unsaturated carbonyl of chalcone were confirmed by X-ray single crystal.
- The 16-benzylidene-modified 2-methoxyestradiol analog **11e** showed a potent antiangiogenic effect.
- Compound **11e** may be a promising antitumour agent with excellent efficacy and low toxicity.
- Compound **11e** may target cancer stem cells and be a potent regulator of angiogenesis and EMT.